A Spectroscopic Analysis of White Dwarfs in the Kiso Survey

M.-M. Limoges and P. Bergeron

Département de Physique, Université de Montréal, C.P. 6128, Succ. Centre-Ville, Montréal, Québec H3C 3J7, Canada.

limoges@astro.umontreal.ca, bergeron@astro.umontreal.ca

ABSTRACT

We present a spectroscopic analysis of white dwarfs found in the Kiso survey. Spectroscopic observations at high signal-to-noise ratio have been obtained for all DA and DB stars in the Kiso Schmidt ultraviolet excess survey (KUV stars). These observations led to the reclassification of several KUV objects, including the discovery of three unresolved DA+DB double degenerate binaries. The atmospheric parameters ($T_{\rm eff}$ and $\log g$) are obtained from detailed model atmosphere fits to optical spectroscopic data. The mass distribution of our sample is characterized by a mean value of 0.606 $M_{\odot}$ and a dispersion of 0.135 $M_{\odot}$ for DA stars, and 0.758 $M_{\odot}$ and a dispersion of 0.192 $M_{\odot}$ for DB stars. Absolute visual magnitudes obtained from our spectroscopic fits allow us to derive an improved luminosity function for the DA and DB stars identified in the Kiso survey. Our luminosity function is found to be significantly different from earlier estimates based on empirical photometric calibrations of M_V for the same sample. The results for the DA stars now appear entirely consistent with those obtained for the PG survey using the same spectroscopic approach. The space density for DA stars with $M_V \leq 12.75$ is 2.80×10^{-4} pc^{-3} in the Kiso survey, which is 9.6% smaller than the value found in the PG survey. The completeness of both surveys is briefly discussed.

Subject headings: stars: fundamental parameters — stars: luminosity function, mass function – white dwarfs

1. Introduction

White dwarf stars represent the final stage of stellar evolution for main sequence stars whose masses lie between 0.07 and 8 $M_{\odot}$, which correspond to about 97% of the stars in the

Galaxy. As the result of the cessation of nuclear reactions, they simply cool off while dissipating the content of their thermal reservoir. Because of these characteristics, the white dwarf luminosity function — the number of white dwarfs as a function of their intrinsic luminosity — is a powerful tool that provides an estimate of the contribution of white dwarf stars to the density of matter in the Galaxy. When the luminosity function is derived from a complete sample of white dwarfs, it contains information such as a direct measure of the stellar death rate in the local galactic disk. The comparison with theoretical evolutionary models (see, e.g., Fontaine et al. 2001) then allows us to measure the age of various components of the Galaxy. Likewise, the mass distribution contains information about the amount of mass lost during the evolution of an initial mass distribution (Liebert et al. 2005, hereafter LBH05).

Luminosity functions have been determined for cool white dwarfs discovered in high proper motion surveys, and through UV color-excess surveys for hot white dwarfs. The cool end of the luminosity function was studied by Liebert et al. (1988) and Leggett et al. (1998), while the hot end was analyzed by Fleming et al. (1986) using white dwarfs identified in the Palomar-Green (PG) survey (Green et al. 1986) and by Darling (1994; see also Wegner & Darling 1994) using the Kiso Schmidt ultraviolet excess survey (KUV). LBH05 have recently improved upon the analysis of Fleming et al. (1986) by applying the spectroscopic method (Bergeron et al. 1992) to measure the effective temperatures and surface gravities of all the DA stars identified in the PG survey. The improved atmospheric parameters allowed a better determination of the absolute visual magnitude (M_V) of each star, and in turn improved the accuracy of the luminosity function calculation. More recently, a similar approach was applied by Harris et al. (2006) to a sample of 6000 white dwarfs (or white dwarf candidates) identified in the Sloan Digital Sky Survey (SDSS) Data Release 3. The luminosity function based on the SDSS extends to redder colors than the PG or Kiso surveys, but does not extend to low enough temperatures to cover the end of the white dwarf cooling sequence, although discoveries made through proper motion diagrams may soon change this picture (Kilic et al. 2006).

In order to measure the luminosity function of white dwarf stars, one needs to carefully define a statistically complete sample. This is a major endeavor, both for common proper motion or UV color excess surveys. Darling (1994) attempted to estimate the completeness of the PG and KUV surveys by counting the number of stars discovered in the overlapping fields of both surveys (see also Section 4.4 below). LBH05 discuss at length the completeness of the PG survey (their Section 4) by comparing their improved luminosity function based on spectroscopic M_V values with the results of Darling (1994) for the KUV survey (see Figure 10 of LBH05). They evaluate the completeness of the PG survey to 75%, while Darling (1994) found a lower value of 58%. However, this comparison between the PG and the Kiso surveys is fundamentally flawed for at least two reasons. First, in the case of the PG survey,

only DA stars are considered while for the Kiso survey, white dwarf stars of *all spectral types* are used in the calculation of the luminosity function. Second, and most importantly, the results of Darling (1994) are based on M_V values determined from empirical photometric calibrations; this is similar to the approach used by Fleming et al. (1986) for the PG survey.

In this paper, we present a study aimed at improving the luminosity function of white dwarf stars by applying the spectroscopic method to the DA and DB stars identified in the Kiso survey. While our primary goal is to improve the comparison of the luminosity functions derived from the PG and Kiso surveys, we also provide an analysis of the global properties of the KUV sample and demonstrate how samples of relatively bright white dwarf stars still hide objects of significant astrophysical interest. Our sample drawn from the Kiso survey is presented in Section 2 and analyzed in Section 3 using the spectroscopic technique. The absolute visual magnitudes obtained from these accurate atmospheric parameter determinations are then used in Section 4 to calculate an improved luminosity function for these stars. A detailed comparison with the results of the PG survey is also presented. Our conclusions follow in Section 5.

2. Spectroscopic Content of the Kiso Survey

The Kiso ultraviolet excess survey (KUV) is a photometric search for UV-excess objects, performed with the 105-cm Schmidt telescope at the Kiso Observatory. A total of 1186 objects were found in 44 fields in a belt from the northern to the southern galactic pole at a galactic longitude of 180 °. The fields of the survey have a mean limiting magnitude of $V = 17.7$ and cover a total area of 1400 square degrees (Noguchi et al. 1980; Kondo et al. 1984).

Our original goal was to secure optical spectroscopic observations for all white dwarfs in the Kiso survey, regardless of their spectral type. Our starting point is the list of objects taken from Table 4.3 of Darling (1994). This list includes 234 white dwarfs identified in the Kiso survey, which at that point in time was only 94% completed (a total of about 250 white dwarfs were expected to be found after completion of the survey). Since cool white dwarfs are difficult to analyze without photometric data, we decided to focus our attention towards the hot end of the sample and exclude from our spectroscopic survey all 15 cool white dwarfs of the DQ, DZ, and DC spectral types. We thus retained a sample of 219 white dwarfs for follow-up spectroscopic observations. Optical spectra for the majority of the objects in this sample were obtained with the Steward Observatory 2.3-m telescope equipped with the Boller & Chivens spectrograph and a Loral CCD detector. The 4.”5 slit together with the 600 l mm^{-1} grating in first order provided a spectral coverage of $\lambda\lambda$3200–5300 at an

intermediate resolution of $\sim$ 6 Å FWHM. The spectra for the remaining southern objects were obtained with the Carnegie Observatories' 2.5-m du Pont telescope at Las Campanas (Chile), equipped with the Boller & Chivens spectrograph and a Tektronic (Tek 5) CCD detector. The 1."5 slit and the 600 l mm^{-1} grating provided a spectral coverage of $\lambda\lambda$3500-6600 at a resolution of $\sim$ 3 Å FWHM. Exposure times were set to reach a signal-to-noise ratio of at least $S/N \sim 50$.

The better resolution and higher S/N of our observations allowed us to revise the spectral classification of many objects in this first sample of 219 stars. At lower resolution, for instance, spectra of B subdwarfs can be easily confused with a DA star (see LBH05 for several examples). We found 30 objects in Darling's sample that turned out to be subdwarfs or main sequence stars, 23 of which have been reclassified as a result of our observations. These 30 objects are displayed in Figure 1 and reported in Table 1, together with references to the original reclassification. Worth mentioning in this figure is KUV 16032+1735, first identified as a magnetic DA white dwarf by Wegner & Swanson (1990). A closer examination of our spectrum reveals no sign of a magnetic field, however, and an attempt to fit this star with our DA model grid suggests an effective temperature above 100,000 K. An independent analysis of this object, which will be reported elsewhere, reveals that KUV 16032+1735 is actually a binary system composed of a hot sdO star and a K-dwarf companion. Additional white dwarfs identified in the KUV survey were also observed as part our spectroscopic follow-up. These are listed in Table 2. None of these were part of the original data set used by Darling (1994), either because they had been discovered afterwards, or for reasons unknown to us. For instance, KUV 14161+2255 (DB) had been reported by Wegner & Swanson (1990) and should have been, in principle, part of Darling's analysis.

Representative DA and DB/DO spectra from our survey are displayed in Figures 2 and 3, respectively, in order of decreasing effective temperature, while magnetic DA white dwarfs are displayed in Figure 4. The He II λ4686 absorption feature is clearly visible in the spectrum of the DAO star KUV 03459+0037 shown in Figure 2. The spectrum for this star was obtained from the SDSS Data Release Web site.[1] Also shown in the same figure are representative DA stars with an unresolved M-dwarf companion (KUV 01162−2311, KUV 03036−0043, KUV 04295+1739); we have a total of six DA+dM systems in our survey. We also show in Figure 3 the spectrum of the DO star KUV 01018−1818 with a very strong He II λ4686 line. Also observed is the presence of Hβ in several DB stars in our sample (DBA stars) as well as Ca II H&K lines (DBZ or DBAZ stars). Discussed further below are three unresolved double-degenerate systems composed of DA+DB white dwarfs that exhibit

[1] http://www.sdss.org/dr7

both hydrogen and helium lines. One of these systems, KUV 02196+2816, has already been analyzed in detail by Limoges et al. (2009). The results for the other systems, KUV 03399+0015 and KUV 14197+2514, are presented in the next section.

Our final spectroscopic sample is thus the combination of the 219 hot white dwarf candidates from Darling (1994), minus the 30 misclassified objects listed in Table 1, to which we add the 7 additional white dwarfs listed in Table 2, for a total of 196 spectroscopically confirmed white dwarfs, three of which are unresolved double degenerates (thus a total of 199 white dwarfs). In summary, we thus have 175 DA stars (including one DAO and 4 magnetics), 23 DB stars, and one DO star.

3. Atmospheric Parameter Determination

Our model atmospheres and synthetic spectra for DA stars are described at length in LBH05 and references therein. These are pure hydrogen, plane-parallel model atmospheres. Non-local thermodynamic equilibrium (NLTE) effects are explicitly taken into account above $T_{\rm eff} = 20,000$ K and energy transport by convection is included in cooler models following the ML2/$\alpha = 0.6$ prescription of the mixing-length theory (see Bergeron et al. 1995). The theoretical spectra are calculated within the occupation formalism of Hummer & Mihalas (1988), which provides a detailed treatment of the level populations as well as a consistent description of bound-bound and bound-free opacities. In order to compare our results directly with those of LBH05, we refrain from using here the new model spectra of Tremblay & Bergeron (2009) that are based on improved Stark profiles for the hydrogen lines; the full implications of these improved models on the spectroscopic analysis of DA stars will be presented elsewhere (Gianninas et al. 2010, in preparation).

Our model atmospheres and synthetic spectra for DB stars are similar to those described in Beauchamp et al. (1996), which include the improved Stark profiles of neutral helium of Beauchamp et al. (1997). Our fitting technique relies on the nonlinear least-squares method of Levenberg-Marquardt (Press et al. 1986), which is based on a steepest descent method. The model spectra (convolved with a Gaussian instrumental profile) and the optical spectrum of each star are first normalized to a continuum set to unity. The calculation of χ^2 is then carried out in terms of these normalized line profiles only. Atmospheric parameters – $T_{\rm eff}$, $\log g$, and $N({\rm H})/N({\rm He})$ for DBA stars – are considered free parameters in the fitting procedure. For DA+dM binaries, Hβ is simply removed from the χ^2 fit when the line is contaminated by the M-dwarf companion.

Atmospheric parameters for the 4 magnetic DA stars displayed in Figure 4 are taken

from the literature: KUV 03292+0035 has a magnetic field of 12 MG (Jordan 1993) and an effective temperature of $T_{\rm eff} \sim 15,500$ K (Schmidt et al. 2003). The value of the magnetic field for KUV 08165+3741 is 9 MG (Angel et al. 1974) with $T_{\rm eff} \sim 11,000$ K (Jordan 2001). Liebert et al. (1985) report 29 MG for KUV 23162+1220 and $T_{\rm eff} \sim 11,000$ K based on *IUE* data. Finally, KUV 23296+2642 has a magnetic field of 2.3 MG, with $T_{\rm eff} = 9400$ K and $\log g = 8.02$ (Bergeron et al. 2001). For the first three magnetic white dwarfs, we simply assume $\log g = 8$.

The DA and DB white dwarfs concealed in DA+DB unresolved double degenerate systems require a special treatment. The first such system discovered in our survey, KUV 02196+2816, was spectroscopically identified as a DBA star by Darling & Wegner (1996) but should have been classified as a DAB star since the hydrogen lines are actually stronger than the helium lines. Limoges et al. (2009) showed that the optical spectrum of this object cannot be reproduced by assuming model atmospheres with a homogeneous hydrogen and helium composition, or even stratified atmospheres, and that the hydrogen and helium lines observed in the spectrum of KUV 02196+2816 can be perfectly reproduced by assuming a double degenerate binary composed of a DA star and a DB star. In this case, the predicted spectrum is obtained by combining pure hydrogen and pure helium model spectra, weighted by their respective radius. The detailed analysis yields $T_{\rm eff} = 27,170$ K and $\log g = 8.09$ for the DA star, and $T_{\rm eff} = 36,340$ K and $\log g = 8.09$ for the DB star. We identified two additional systems in our spectroscopic survey, KUV 03399+0015 and KUV 14197+2514. KUV 03399+0015 was first identified as a DA? by Darling & Wegner (1994), and later as a DAB by Eisenstein et al. (2006), while KUV 14197+2514 was classified as a DBA star by Wegner & Swanson (1990). An analysis similar to that of KUV 02196+2816 of these two objects reveals that both spectra cannot be reproduced with single-star models, and that the hydrogen and helium line profiles can only be explained by assuming a composite DA+DB double degenerate model. Figure 5 summarizes our results for the three systems. A more detailed analysis of these binaries will be presented elsewhere (Limoges & Bergeron 2010, in preparation).

The atmospheric parameters for the white dwarfs in our sample — 192 single stars and 6 from the binary systems of Figure 5 — are reported in Tables 3 and 4 for the DA and DB stars, respectively; we exclude from our analysis the DO star KUV 01018−1818 since we have no models to analyze this object properly. The values in parentheses represent the uncertainties of each parameter, calculated by combining the internal error obtained from the covariance matrix and the external error estimated for DA stars at 1.2% in $T_{\rm eff}$ and 0.038 dex in $\log g$ (see LBH05 for details); we assume the same uncertainties for DB stars. The hydrogen abundances in Table 4 are provided for DBA stars only, otherwise a pure helium composition is assumed. The stellar mass (M) and the white dwarf cooling time ($\log \tau$,

where τ is measured in years) are obtained from detailed evolutionary cooling sequences appropriate for these stars. For DA stars with $T_{\rm eff} > 30,000$ K, we use the carbon-core cooling models of Wood (1995) with thick hydrogen layers of $q({\rm H}) \equiv M_{\rm H}/M_\star = 10^{-4}$ and $q({\rm He}) = 10^{-2}$, while for $T_{\rm eff} < 30,000$ K, we use cooling models similar to those described in Fontaine et al. (2001) but with carbon-oxygen cores. For DB stars, we rely on similar models but with thin hydrogen layers of $q({\rm H}) = 10^{-10}$ representative of helium-atmosphere white dwarfs. The absolute visual magnitude (M_V) and luminosity (L) of each star are calculated using the prescription of Holberg & Bergeron (2006)[2], while the apparent V magnitudes are taken from the catalog of McCook & Sion (2006). The $1/v_{\rm max}$ value corresponds to the maximum volume in which it is possible to find a particular white dwarf given a limiting apparent V magnitude of the survey; this will be discussed further in Section 3.5. Note that the $1/v_{\rm max}$ value is provided only for white dwarfs in our statistically complete sample defined below.

The global properties of the DA and DB stars in the KUV sample are summarized in Figure 6 in a mass versus effective temperature diagram. This figure indicates that the majority of our DA stars have effective temperatures between $T_{\rm eff} \sim 10,000$ K and 25,000 K. Only 13 stars in our sample have temperatures below 10,000 K; the coolest object is KUV 23235+2536 with $T_{\rm eff} = 5930$ K. An examination of Figure 6 reveals the well-known problem where the spectroscopic masses for DA stars show a significant increase below $T_{\rm eff} \sim 13,000$ K (see also LBH05). Various explanations have been proposed to account for this phenomenon (Bergeron et al. 2007; Koester et al. 2009), although to this date none are completely satisfactory. The most promising solution to this problem, namely a mild and systematic helium contamination from convective mixing that would mimic the high $\log g$ spectroscopic measurements, has recently been ruled out by Tremblay et al. (2010) who reported extremely low upper limits of the helium abundance in several cool DA white dwarfs using high-resolution spectra from the Keck I 10-m telescope. Figure 6 also reveals that near $\sim 15,000$ K, 4 DB stars have significantly higher masses than the rest of the DB sample. This particular trend at low effective temperatures has been observed in other analyses as well (see, e.g., Fig. 5 of Kepler et al. 2007 for the DB stars identified in the SDSS) and this problem is usually attributed to uncertainties in the treatment of van der Waals broadening of neutral helium lines (Beauchamp et al. 1996). In the results shown here, however, DB stars with normal masses ($\sim 0.6\ M_\odot$) are also found in the same range of temperatures. To illustrate this more clearly, we show in Figure 7 our best fits to two DB stars near 15,000 K, but with significantly different $\log g$ values. In this particular range of temperatures, the He I λ3820 and λ4388 lines are the most gravity sensitive and the

[2]See http://www.astro.umontreal.ca/~bergeron/CoolingModels.

strengths of these lines do indeed appear very different in both stars. We emphasize that this result for DB stars is completely independent of any modeling of the line profiles and we must therefore conclude that the spread in mass observed in Figure 6 may thus be real after all. Perhaps the massive DB stars observed here represent the descendants of the new class of white dwarf stars with carbon-rich atmospheres discovered by Dufour et al. (2007, 2008). Indeed, the coolest 'hot DQ' stars have temperatures near $\sim 18,000$ K, below which they are presumably transformed into something else. Small amounts of helium thoroughly mixed in their atmospheres could easily reappear at the surface of these stars below 18,000 K or so, turning them into DB stars in a process similar to the transformation of hot DO (or even DAO) stars into DA stars near $\sim 45,000$ K.

The mass distribution is shown in Figure 8 for the 136 DA stars above 13,000 K (i.e., above the temperature where the masses of DA stars are reliable) as well as for the 23 DB white dwarfs. The mass distribution of DA stars has a mean value of 0.606 $M_{\odot}$ with a dispersion of 0.135 $M_{\odot}$. These values are very similar to those obtained by LBH05 for the DA stars in the PG sample (0.603 and 0.134 $M_{\odot}$, respectively) in the same temperature range. The mean mass for the DB stars in the KUV sample is 0.758 $M_{\odot}$, a value significantly larger than that for the DA stars; the dispersion is also much larger. The mass distribution for the DB stars appears rather flat compared to those presented in Beauchamp et al. (1996, 54 DB stars) or in Voss et al. (2007, 71 DB stars), although the number of DB stars in our sample is admittedly smaller than in these two previous studies. We note finally that we found no low mass ($M < 0.5$ $M_{\odot}$) DB white dwarfs in our sample, in agreement with the results of Beauchamp et al. (1996).

4. Luminosity Function

4.1. General Considerations

We can now proceed to calculate the luminosity function of DA and DB stars in the Kiso survey. Since we will compare our results with those of Darling (1994) and with the PG survey (LBH05), it is relevant to provide here some details of how these calculations are performed. The luminosity function is obtained following the $1/v_{\rm max}$ method, originally developed by Schmidt (1968) in the context of quasars. This method requires that we determine for each star the maximum volume, $v_{\rm max}$, in which the object would have been detected given the limiting magnitude of the survey. The distance to each star can be directly obtained from the apparent and absolute V magnitudes. Since the stars are not uniformly distributed in the direction perpendicular to the galactic disk, but instead follow an exponential disk, we define a weighted volume $dv' = \exp(-z/z_0)\, dv$, where $z = r \sin\theta$ is the distance of the object

from the galactic plane, z_0 is the galactic disk scale height, and θ is the absolute value of the galactic latitude of the object. Here we assume $z_0 = 250$ pc as in LBH05.

The Kiso survey is a magnitude-limited survey, which implies that it must be complete down to a given limiting magnitude $V_{\rm lim}$. For a given star with a magnitude V, $V_{\rm lim}$ defines a maximum distance $d_{\rm max}$ at which an object could have been observed and still have been found in the survey. This in turn defines the maximum volume, $v_{\rm max}$. As mentioned in Green (1980), however, each photographic plate has a different limiting magnitude. It was then proposed to define a maximum volume for each field. The total maximum volume for a given star is thus the sum of all the small individual volumes. Also, in the case where two fields or more overlap, the area of overlap is given to the field with the fainter limiting magnitude. We finally obtain for each star

$$v_{\rm max} = \sum_{j=1}^{n_f} \frac{\omega_j}{4\pi} \int_0^{d_{\rm max}} e^{-z/z_0}\ 4\pi r^2 dr \tag{1}$$

where n_f is the total number of fields. Since ω_j represents the area covered by each field, $\sum_{j=1}^{n_f} \omega_j$ must be equal to the total area covered by the survey (in steradians). The limiting magnitude can be calculated following the $v/v_{\rm max}$ test of uniformity of Schmidt (1968). The method states that a sample is complete when the average value of $v/v_{\rm max}$ is equal to 0.5. Once the value of $V_{\rm lim}$ that satisfies this constraint has been found, all white dwarfs with V fainter than $V_{\rm lim}$ must be removed from the sample. The remaining stars define the complete sample from which the luminosity function can be derived.

Since $v_{\rm max}$ represents the volume within which it is possible to find a particular white dwarf, the contribution of each star to the local space density is then simply given by $1/v_{\rm max}$ (Schmidt 1968). The differential luminosity function as a function of M_V can finally be obtained by summing all the individual contributions to the local space density:

$$\phi(M_V) = \sum_{i=1}^{n_b} 1/v_{{\rm max}_i} \tag{2}$$

where n_b is the number of stars in each magnitude bin of the complete sample. The uncertainties are evaluated as if the stars were distributed randomly in space. The statistical uncertainty in each bin is then given by $\sigma_\phi = [\sum_{i=1}^{n_b} (1/v_{{\rm max}_i})^2]^{1/2}$ (Boyle 1989).

4.2. The Luminosity Function from Darling (1994)

In the next section, we will compare our luminosity function of DA and DB stars based on spectroscopic estimates of M_V with the results of Darling (1994) based on empirical photometric calibrations of M_V. Prior to this, we must first demonstrate that we are able to reproduce the luminosity function displayed in his Figure 4.2 (also reproduced in Figure 10 of LBH05) using the V and M_V values provided in his Table 4.3. Note in this case that the luminosity function is calculated using all 234 white dwarf stars identified in the Kiso survey, all spectral types included. His method is identical to that described above with the only exception that there is no explicit sum over all fields in equation (1). Instead, the area of each field is assumed to be constant, in which case a single factor $\omega/4\pi$ appears in the equation, where ω for the Kiso survey is 1400 square degrees (or ~ 0.43 steradians). We know that in Wegner & Darling (1994), the luminosity function was scaled by a certain factor to account for the fact that the Kiso survey was not complete at that time. In Darling (1994), this factor had a value of 1186/1115 since the Kiso survey was only 94% complete. This correction factor is included in all our calculations below.

The comparison of the results between Darling's calculations and ours using the same stars, as well as V and M_V values, is displayed in Figure 9. Both functions have the same exact shape but ours is scaled downwards by a factor of ~ 2.5, which suggests a constant correction factor between both calculations. We also note that our calculation of the limiting magnitude of the survey using this sample agrees perfectly with the value obtained by Darling, $V_{\rm lim} = 17.35$. As it is not stated explicitly in Darling (1994) that his luminosity function contains a correction factor (to account for other types of incompleteness, for instance), we ignore the source of the difference between our calculations and Darling's and use our method of calculation in the remainder of this paper[3]. We must finally mention that the code we are using here is the same as that used by LBH05 so the comparisons discussed below will be entirely consistent.

4.3. An Improved Luminosity Function for KUV White Dwarfs

The main goal of our spectroscopic survey is to improve upon the luminosity function of Darling (1994) by using spectroscopic values of M_V rather than empirical photometric calibrations. The absolute magnitudes are central to the calculation of the luminosity func-

[3]We also contacted G.W. Darling directly and attempted to figure out the discrepancy but the original calculations are lost in the sands of time.

tion and it is crucial to measure M_V values as accurately as possible. In Darling (1994), M_V values were assigned for 125 stars (out of 234) with measured $(B-V)$ using empirical $(B-V)$ vs. M_V relations derived by Sion & Liebert (1977) and Dahn et al. (1982) for hot and cool white dwarfs, respectively. Additional M_V values for 9 objects were directly taken from McCook & Sion (1987). Finally, a linear fit based on measured photometric $(B-V)$ and photographic $(m_U - m_G)$ color indices was then used to assign approximate $(B-V)$ values, and thus M_V values, to the remaining 100 stars without $(B-V)$ or M_V measurements. In reality, this relation is far from being linear and a substantial dispersion is present in the data (see Figure 4.1 of Darling 1994), potentially introducing a significant uncertainty in the M_V estimates.

Our spectroscopic M_V values taken from Tables 3 and 4 are compared in Figure 10 with those derived by Darling (1994) for the 192 white dwarf stars in common. In doing so, we explicitly excluded from Darling's sample all objects that have been spectroscopically misclassified in the Kiso survey (Table 1 and Figure 1). The double degenerate binary components are compared with Darling's results for a single DAB/DBA star. The differences observed are quite significant, with the empirical estimates being generally fainter than the spectroscopic values. In some cases, the differences can reach 2 to 3 magnitudes. It is therefore expected that the corresponding luminosity functions based on these absolute magnitudes will be affected as well.

With the spectroscopic M_V values for our sample of 175 DA and 23 DB stars provided in Tables 3 and 4 respectively, we can now proceed to the evaluation of the luminosity function. The first step is to find the limiting magnitude of the survey following the $v/v_{\rm max}$ method described above. We find $V_{\rm lim} = 17.41$, which defines a complete sample of 168 white dwarf stars (149 DA and 19 DB stars). This complete sample is flagged in Tables 3 and 4 by a value of $1/v_{\rm max}$ in the appropriate column (otherwise the field is empty). The luminosity function is then simply computed by summing these values in appropriate bins (see equation 2), in this case half-magnitude bins.

We first compare our improved luminosity function with that of Darling (1994) by using the same subset of 192 stars shown in Figure 10, (i.e. misclassified objects from Darling's sample and the additional white dwarfs from Table 2 are not taken into account). Even though the stars used in the comparison are the same, the absolute magnitudes in each sample are evaluated differently, and so are the limiting magnitudes. We find using Darling's M_V values a limiting magnitude of $V_{\rm lim} = 17.35$, which defines a complete sample of 161 objects, while our spectroscopic M_V values yield $V_{\rm lim} = 17.41$ for a complete sample of 164 objects. The corresponding luminosity functions are compared in Figure 11. Despite the large differences in M_V values observed in Figure 10, the differences in the luminosity

functions do not appear as significant, with the noticeable exception of the 9.5, 12.5, and 13.0 magnitude bins. A similar conclusion was reached by LBH05 when comparing the luminosity function of PG stars with the earlier estimates of Fleming et al. (1986). We must note that the main effect here is to shift the number of stars from one bin to another. For instance, the largest difference observed is near the peak of the luminosity function where our determination based on spectroscopic M_V values is lower than that of Darling. Indeed, a lot of the objects in these magnitude bins in Darling's analysis have been shifted to brighter bins as a result of his overestimates of M_V values (see Figure 10). We finally note that the last two bins at $M_V = 14.0$ and 14.5 are populated by only one star each (KUV 23235+2536 and KUV 08275+3252, respectively). The Kiso survey is obvioulsy very imcomplete in this region and we decided to remove these two white dwarfs from our sample in the remainder of our analysis[4].

In Figure 10 of LBH05, the authors compare their luminosity function for DA stars in the PG survey with the results of Darling (1994), which, as mentioned above, also contains the contributions from other spectral types. In order to improve this comparison, we derived an independent KUV luminosity function for DA stars only, by simply removing the DB white dwarfs from our sample (DB stars account for 17.3% of our complete sample). It is now possible to make a detailed comparison with the luminosity function obtained by LBH05, which is based on the exact same analysis, including model atmospheres, observing setup, fitting technique, and luminosity function calculations. As mentioned explicitly in LBH05, their luminosity function did not undergo any correction, as is the case with ours. It is then possible to compare the results from both functions directly, as shown in Figure 12. The first result is that both luminosity functions agree much better than estimated by LBH05, who concluded, based on the results shown in their Figure 10, that "the KUV luminosity function has significantly more stars than PG in the bins M_V 10.5 to 13.0, with the PG appearing to become incomplete by a factor of 4 in the 12.0 and the two fainter magnitude bins". The comparison shown here indicates on the contrary that both functions agree perfectly within the error bars in these particular bins. However, there appears to be a deficiency of luminous white dwarfs ($M_V \leq 10$) in the Kiso survey. It is perhaps not surprising that the luminosity functions from the PG and Kiso surveys are so similar, since the detection method is the same (UV excess). So whatever incompleteness factors affect the PG survey seem to affect the Kiso survey as well.

Another way to compare both luminosity functions is to calculate the local space densities of white dwarfs, which can be simply obtained by integrating the luminosity function

[4]KUV 23235+2536 has an estimated temperature of only $T_{\rm eff} = 5930$ K, and it is difficult to understand how such a cool object ended up in a UV color-excess survey!

over a given range of M_V. For $M_V < 12.75$, we obtain 2.80×10^{-4} pc^{-3} while LBH05 report a value[5] of 3.07×10^{-4} pc^{-3} in the same magnitude interval, or a value only 9.6% larger than our estimate. The Kiso survey thus appears to be *less complete*, if anything, than the PG survey in that range of absolute visual magnitude. The Kiso survey is certainly deeper than PG, and it should thus be more complete for fainter magnitude bins since the PG survey is known to be fairly incomplete at the faint end of the luminosity function (LBH05). We note, however, that the differences do not appear as large as previously estimated by LBH05, as discussed above.

Finally, our final luminosity function for the Kiso white dwarfs, including all 149 DA and 19 DB stars in the complete sample, is displayed in Figure 13. We obtain from the sum of all magnitude bins a local space density of white dwarfs in the Kiso survey of 5.49×10^{-4} pc^{-3}. Of course, the Kiso sample does not extend to the faint magnitudes where the peak of the luminosity function occurs ($M_V \sim 15.5$), and the space density determined here accounts for only $\sim 11\%$ or less of the total space density of white dwarf stars, which is estimated at 5×10^{-3} pc^{-3} or so. For completeness, we also compare in Figure 14 our luminosity function with the results obtained by Harris et al. (2006) and DeGennaro et al. (2008) for the white dwarfs discovered in the SDSS (Data Release 3). Our luminosity function is plotted here as a function of $M_{\rm bol}$ to be consistent with the SDSS determinations. Our results agree fairly well, within the uncertainties, with the results of DeGennaro et al. for magnitude bins between $M_{\rm bol} = 7.5$ and 11.5 (with a few notable exceptions), but appear seriously underestimated for brighter and fainter magnitude bins.

4.4. Completeness of the PG and Kiso Surveys

By counting the number of KUV white dwarfs (all spectral types included) found by the PG survey in the overlapping fields (600 square degrees of overlap) and within the magnitude limit of the PG survey, Darling (1994) estimated the completeness of the PG survey to 57.5%, or 60.5% if white dwarfs not in the statistically complete PG sample are also included. However, as discussed in Section 2, many KUV white dwarfs turn out to be lower gravity objects. A similar estimate of the completeness of the PG survey based on our spectral reclassification of DA and DB stars yields instead a value of 67.6%.

Darling (1994) also used the PG survey to estimate the completeness of the Kiso survey by turning the problem around, and by counting the number of PG stars in the overlapping

[5]LBH05 actually give a value of 5.0×10^{-4} pc^{-3} but this number is inaccurate for reasons unknown to one of the co-authors of both studies (P.B.) who obtained the correct number provided here.

fields, all spectral types included, that were actually missed in the Kiso survey. While the Kiso survey is much deeper ($V_{\rm lim} \sim 17.35$) than the PG survey ($V_{\rm lim} \sim 16.16$), only 74.2% of the white dwarfs in the overlapping fields of the PG survey were recovered in the Kiso survey! Since none of the new KUV stars (Table 2) are part of the PG sample, this estimate is still valid. Once again, using only our spectroscopically confirmed sample of DA and DB stars, we find instead a value of 84.4% for the completeness of the Kiso survey. Given the results shown in Figure 12, it is likely that both the PG and Kiso surveys suffer from a comparable level of incompleteness. We refer the reader to the additional discussion of LBH05 (Section 4) regarding the completeness of the PG survey. Obviously, deeper and more complete surveys are still badly needed.

The Sloan Digital Sky Survey (SDSS) is certainly among the most important developments in the last few years in terms of observational data of white dwarf stars since the PG survey. The SDSS is looking at 10,000 deg^2 of high-latitude sky in five bandpasses ($ugriz$) and is producing images in these five bandpasses from which galaxies, quasars, and stars are selected for follow-up spectroscopy. The selection effects in this survey are important, as discussed in Kleinman et al. (2004) and Eisenstein et al. (2006), and therefore, it cannot be considered as a complete survey in any sense. For instance, DeGennaro et al. (2008) found a completeness of 51% for their uncorrected sample of white dwarfs from the SDSS, which is mainly composed of DA stars. Also, the S/N of the SDSS spectra is known to be proportional to the brightness of the object, since the integration time is fixed. This can lead to large uncertainties in the determination of the atmospheric parameters of fainter objects (Gianninas et al. 2005). Finally, as mentioned in Eisenstein et al. (2006), "completeness is not our goal", since they know that white dwarfs with $T_{\rm eff} \lesssim 8000$ K are lost because of the color-cut, and that magnetic white dwarfs can pass through the detection system without being noticed. DeGennaro et al. (2008) are in possession of a much larger sample than ours, which allows them to divide their luminosity function into several mass components. However, when conducting a statistical analysis of a sample, the completeness of this sample should be a crucial parameter if the results are to be interpreted physically.

5. Conclusion

We presented an analysis of the DA and DB white dwarfs in the KUV survey, and determined the atmospheric parameters for each star from detailed model atmosphere fits to optical spectroscopic data. The M_V values derived from the atmospheric parameters were compared with those of Darling (1994), which were obtained from photometric empirical calibrations. Our study allowed us to measure directly the impact of the use of state-of-

the-art model atmospheres on the determination of absolute magnitudes for white dwarfs. The differences were found to be significant, but had a somewhat smaller impact on the calculation of the luminosity function.

We then proceeded to derive the luminosity function of DA and DB stars found in the Kiso survey. We find as a result of our improved M_V values a smaller number of stars in the fainter magnitude bins than estimated by Darling (1994). The comparison of our luminosity function with that of LBH05, for DA stars only, reveals that both functions are similar. We obtained a local space density of white dwarfs of 5.49×10^{-4} pc^{-3}, while this number drops to 2.80×10^{-4} pc^{-3} for $M_V \leq 12.75$. These results are now entirely consistent with those published in LBH05 for the PG survey and the completeness of both surveys appears comparable.

Our spectroscopic survey of white dwarfs in the Kiso survey has also led to an important spectral reclassification of the sample published in Darling (1994). In particular, we have identified three unresolved double degenerate binaries. A two-component fit confirmed that KUV 02196+2816, KUV 03399+0015, and KUV 14197+2514 are unresolved double degenerate binaries composed of a DA and a DB star. These systems were easily identified in our analysis because both components had different spectral types. However, double degenerates composed of two DA stars would go totally unnoticed, as demonstrated by Liebert et al. (1991). One may wonder how many such binaries might be hiding in spectroscopic surveys such as KUV or PG. This in turn could affect our determination of the true space density of white dwarf stars.

This era of large scale surveys where the samples can contain up to thousands of stars will certainly help us in the characterization of our Galaxy. Accurate statistical analyses will then provide even more precise determinations of, for example, the white dwarf space densities in the different populations of the Galaxy, the stellar contribution to the mass of the Galaxy, the age of the local galactic disk, the stellar formation and death rates, etc. The issue of completeness is thus of great importance when statistical analyses of these samples are considered.

We would like to thank the director and staff of Steward Observatory and Carnegie Observatories for the use of their facilities. We would also like to thank A. Gianninas for the acquisition of the spectra in the southern hemisphere and for a careful reading of this manuscript. This work was supported in part by the NSERC Canada and by the Fund FQRNT (Québec). P.B. is a Cottrell Scholar of Research Corporation for Science Advancement.

REFERENCES

Angel, J.R.P., Carswell, R., Strittmatter, P.A., Beaver, E.A., & Harms, R. 1974, ApJ, 194, L47

Beauchamp, A., Wesemael, F., & Bergeron, P. 1997, ApJS, 108, 559

Beauchamp, A., Wesemael, F., Bergeron, P., Liebert, J., & Saffer, R. A. 1996, in ASP Conf. Ser. Vol. 96, Hydrogen-Deficient Stars, ed. S. Jeffery & U. Heber (San Francisco: ASP), 295

Bergeron, P., Gianninas, A., & Boudreault, S. 2007, in Proc. 15th European Workshop on White Dwarfs, ed. R. Napiwotzki & M. Burleigh (San Francisco: ASP), 372, 29

Bergeron. P., Leggett, S.K., & Ruiz, M.T. 2001, ApJS, 133, 413

Bergeron, P., Saffer, R.A., & Liebert, J. 1992, ApJ, 394, 247

Bergeron, P., Wesemael, F., Lamontagne, R., Fontaine, G., Saffer, R.A., & Allard, N.F. 1995, ApJ, 449, 258

Boyle, B.J. 1989, MNRAS, 240, 533

Dahn, C.C., Harrington, R.S., Riepe, B.Y, Christy, J.W., Guetter, H.H., Kallarakal, V.V., Miranian, M., Walker, R.L., Vrba, F.J., Hewitt, A.V., Durham, W.S., & Ables, H.D. 2001, AJ, 87, 419

Darling, G.W. 1994, PhD thesis, Dartmouth College

Darling, G.W., & Wegner, G. 1994, ApJ, 108, 2025

Darling, G.W., & Wegner, G. 1996, ApJ, 111, 685

DeGennaro, S., von Hippel, T., Winget, D.E., Kepler, S.O., Nitta, A., Koester, D., & Althaus, L. 2008, AJ, 135, 1

Dufour, P., Fontaine, G, Liebert, J., Schmidt, G.D., & Behara, N. 2008, ApJ, 683, 978

Dufour, P., Liebert, J., Fontaine, G, & Behara, N. 2007, Nature, 450, 522

Eisenstein, D.J., et al. 2006, ApJS, 167, 40

Fleming, T.A, Liebert, J., & Green, R.F. 1986, ApJ, 308, 176

Fontaine, G., Brassard, P., & Bergeron, P. 2001, PASP, 113, 409

Gianninas, A., Bergeron, P., & Fontaine, G. 2005, ApJ, 631, 1100

Green, R.F. 1980, ApJ, 238, 685

Green, R. F., Schmidt, M., & Liebert, J. 1986, ApJS, 61, 305

Harris, H.C., et al. 2006, AJ, 131, 571

Holberg, J.B., Barstow, M.A., & Burleigh, M.R. 2003, ApJS, 147, 145

Holberg, J.B., & Bergeron, P. 2006, ApJ, 132, 1221

Hummer, D.G., & Mihalas, D. 1988, ApJ, 331, 794

Jordan, S. 1993, in White Dwarfs: Advances in Observation and Theory, NATO ASI Series, ed. M. A. Barstow (Dordrecht: Kluwer Academic Publishers), 333

Jordan, S. 2001, in ASP Conf. Ser. Vol. 226, 12th European Workshop on White Dwarfs, eds. J. L. Provencal, H. L. Shipman, J. MacDonald, & S. Goodchild, 269

Kawka, A., & Vennes, S. 2005, in ASP Conf. Ser. Vol.334, 14th European Workshop on White Dwarf Stars, eds. Koester, D., Moehler, S., 101

Kawka, A., Vennes, S., & Thorstensen, J.R. 2004, AJ, 3, 1702

Kepler, S.O., Kleinman, S.J., Nitta, A., Koester, D., Castanheira, B.G., Giovannini, O., Costa, A.F.M., & Althaus, L. 2007, MNRAS, 375, 1315

Kidder, K.M. 1991, PhD thesis, University of Arizona

Kilic, M., Munn, J.A., Harris, H.C., Liebert, J., von Hippel, T., Williams, K.A., Metcalfe, T.S., Winget, D.E., & Levine, S.E. 2006, AJ, 131, 582

Kleinman, S.J., et al. 2004, ApJ, 607, 426

Koester, D., Kepler, S.O., Kleinman, S.J., & Nitta, A. 2009, in 16th European White Dwarfs Workshop, Journal of Physics: Conference Series, Vol. 172, 2006

Kondo, M., Noguchi, T., & Maehara, H. 1984, Ann. Tokyo Astron. Obs., 20, 130

Lamontagne, R., Demers, S., Wesemael, F., Fontaine, G., & Irwin, M.J. 2000, AJ, 119, 241

Leggett, S.K., Ruiz, M.T., & Bergeron, P. 1998, ApJ, 497, 294

Liebert, J., Bergeron, P., & Holberg, J.B. 2005, ApJ, 156, 47 (LBH05)

Liebert, J., Bergeron, P., & Saffer, R.A. 1991, in 7th European Workshop on White Dwarfs, NATO ASI Series, ed. G. Vauclair & E. M. Sion (Dordrecht: Kluwer Academic Publishers), 409

Liebert, J., Dahn, C.C., & Monet, D.G. 1988, ApJ, 332, 891

Liebert, J., Schmidt, G.D., Sion, E.M., Starrfield, S.G., Green, R.F., & Boroson, T.A. 1985, PASP, 97, 158

Limoges, M.-M., Bergeron, P., & Dufour, P. 2009, ApJ, 696, 1461

Lisker, T., Heber, U., Napiwotzki, R., Christlieb, N., Han, Z., Homeier, D., & Reimers, D. 2005, A&A, 430, 223

McCook, G.P., & Sion, E.M. 1987, ApJS, 65, 603

McCook, G.P., & Sion, E.M. 2006, VizieR Online Data Catalog, 3235

Noguchi, T., Maehara, H., & Kondo, M. 1980, Ann. Tokyo Astron. Obs., 18, 55

Press, W. H., Flannery, B. P., Teukolsky, S. A., & Vetterling, W. T. 1986, Numerical Recipes (Cambridge: Cambridge University Press)

Schmidt, M. 1968, ApJ, 151, 393

Schmidt, G.D., et al. 2003, ApJ, 595, 1101

Sion, E.M., & Liebert, J. 1977, ApJ, 213, 468

Stroeer, A., Heber, U., Lisker, T., Napiwotzki, R., Dreizler, S., Christlieb, N., & Reimers, D. 2007, A&A, 462, 269

Tremblay, P.-E., & Bergeron, P. 2009, ApJ, 696, 1755

Tremblay, P.-E., Bergeron, P., Kalirai, J.S., & Gianninas, A. 2010, ApJ, 712, 1345

Voss, B., Koester, D., Napiwotzki, R., Christlieb, N., & Reimers, D. 2007, A&A, 470, 1079

Wagner, M.R., Sion, E.M., Liebert, J., Starrfield, S.G., & Zotv, N. 1986, PASP, 98, 552

Wegner, G., & Darling, G. W. 1994, in Stellar and Circumstellar Astrophysics, eds.G. Wallerstein & A. Noriega-Crespo, ASP Conf. Series No. 57 (San Francisco CA: Astronomical Society of the Pacific), 178

Wegner, G., & Swanson, S.R. 1990, AJ, 99, 330

Wood, M. A. 1995, in 9th European Workshop on White Dwarfs, NATO ASI Series, eds. D. Koester & K. Werner (Berlin: Springer), 41

Table 1. Misclassified Objects

KUV	WD	ST (Darling 1994)	ST (this work)	Notes
00486−2016	0048−202	DA	sdB	1
01098−2629	0109−264	DA	sdB	1
01134−2423	0113−243	DA	sdB	2
01542−0710	0154−071	DA?	sdB	1
02222+3124	0222+314	DA	sdB	2
02409+3407	0240+341	DA	MS	2
04473+1737	0447+176	DB	sdOB	2
05097+1649	0509+168	DA	MS	3
05101+1619	0510+163	DA	MS	2
05260+2711	0526+271	DA	sdB	2
05296+2610	0529+261	DA	sdB	2
06274+2958	0627+299	DA	sdB	2
06289+3126	0628+314	DA	sdB	2
07528+4113	0752+412	DA?	sdB	2
09272+3854	0927+388	DA	sdB	2
09306+3740	0930+376	DA	sdB	2
09327+3937	0932+396	DA	sdB	2
09339+3821	0933+383	DA	sdB	4
09372+3933	0937+395	DA	sdB	2
09436+3709	0943+371	DA	sdB	2
09467+3809	0946+381	DA	sdB	2
12562+2839	1256+286	DA?	sdB	2
13024+2824	1302+284	DA	sdB	4, 5
13023+3145	1302+317	DB	sdOB	2
13046+3118	1304+313	DA	sdB	2
16032+1735	1603+175	DA	sdO+dK	2
16118+3906	1611+390	DA	sdB	2
18169+6643	1816+667	DB	sdOB	2
22585+1533	2258+155	DB	sdO	6
23099+2548	2309+258	DA	sdB	2

Note. — Note. – (1) Lisker et al. 2005; (2) this work; (3) Kawka et al. 2004; (4) Not in McCook and Sion; (5) Holberg et al. 2003; (6) Stroeer et al. 2007.

Table 2. Additional KUV White Dwarfs

KUV	WD	ST	Reference
01018−1818	0101−182	DO	Lamontagne et al. (2000)
03439−0048	0343−007	DA	Wagner et al. (1986)
03459+0037	0345+006	DAO	Eisenstein et al. (2006)
08422+3813	0842+382	DA	Kawka & Vennes (2005)
14161+2255	1416+229	DB	Wegner & Swanson (1990)
18004+6836	1800+685	DA	Kidder (1991)
18453+6819	1845+683	DA	Kidder (1991)

Table 3. Atmospheric Parameters of DA Stars from the KUV Sample

KUV	WD	$T_{\rm eff}$	(K)	log g	$M/M_\odot$	M_V	log $L/L_\odot$	V	D(pc)	$1/v_{\rm max}$	log τ	Notes
00300−1810	0030−181	13,640	(362)	7.81 (0.06)	0.51 (0.00)	11.18	−2.17	16.8	133	1.78(−6)	8.30	
00328−1735	0032−175	9830	(142)	8.18 (0.05)	0.71 (0.00)	12.53	−2.97	14.9	29	9.92(−6)	8.91	
00329−1747	0032−177	16,780	(281)	7.83 (0.05)	0.52 (0.00)	10.83	−1.82	15.7	94	1.16(−6)	8.00	
00334−1738	0033−176	23,030	(477)	7.98 (0.06)	0.62 (0.00)	10.49	−1.35	17.6	264	—	7.51	
00337−1749	0033−178	24,310	(572)	7.26 (0.08)	0.34 (0.00)	9.25	−0.79	17.7	489	—	7.24	
00442−2156	0044−219	11,890	(207)	7.84 (0.07)	0.51 (0.00)	11.47	−2.43	17.26	143	2.55(−6)	8.49	
00582−1834	0058−185	17,760	(335)	8.02 (0.06)	0.63 (0.00)	11.02	−1.83	17.26	177	1.46(−6)	8.07	
01024−1836	0102−185	72,370	(1793)	7.16 (0.08)	0.48 (0.00)	7.13	+1.35	16.9	900	2.61(−8)	5.07	
01071−1917	0107−192	14,750	(254)	7.83 (0.05)	0.52 (0.00)	11.06	−2.04	16.3	111	1.53(−6)	8.20	
01138−2431	0113−245	56,370	(1975)	7.58 (0.13)	0.54 (0.00)	8.29	+0.55	17.67	751	—	6.15	
01157−2546	0115−257	14,990	(264)	7.94 (0.05)	0.58 (0.00)	11.19	−2.08	16.90	138	1.80(−6)	8.25	
01162−2311	0116−231	31,430	(489)	7.65 (0.06)	0.49 (0.00)	9.30	−0.57	15.63	184	1.98(−7)	6.90	1
01246−2546	0124−257	24,110	(392)	7.73 (0.05)	0.50 (0.00)	10.03	−1.11	15.66	133	4.48(−7)	7.28	
01308−2721	0130−273	22,490	(376)	7.92 (0.05)	0.58 (0.00)	10.44	−1.35	16.93	198	7.24(−7)	7.50	
01491−1127	0149−114	9120	(137)	8.03 (0.07)	0.62 (0.00)	12.59	−3.01	16.6	63	1.07(−5)	8.90	
01498−1227	0149−124	12,180	(199)	8.28 (0.05)	0.78 (0.00)	12.05	−2.65	17.2	106	5.33(−6)	8.73	
01518−0928	0151−094	26,000	(460)	7.75 (0.06)	0.51 (0.00)	9.89	−0.99	17.7	364	—	7.16	
01552−0703	0155−070	10,690	(165)	8.09 (0.06)	0.66 (0.00)	12.10	−2.76	16.2	66	5.69(−6)	8.76	
01595−1109	0159−111	11,140	(174)	8.22 (0.06)	0.74 (0.00)	12.18	−2.77	16.9	87	6.30(−6)	8.80	
02185+2923	0218+293	17,110	(292)	8.15 (0.05)	0.71 (0.00)	11.27	−1.98	17.50	176	—	8.23	
02196+2816	0219+282A	27,170	(383)	8.09 (0.04)	0.69 (0.00)	10.32	−1.12	18.16	369	—	7.25	2
02245+3145	0224+317	14,550	(330)	7.77 (0.06)	0.49 (0.00)	11.00	−2.04	16.9	151	1.42(−6)	8.18	
02292+2704	0229+270	24,270	(374)	7.88 (0.05)	0.57 (0.00)	10.24	−1.19	15.58	116	5.72(−7)	7.31	
02295+3529	0229+354	12,860	(385)	7.78 (0.07)	0.49 (0.00)	11.26	−2.26	16.90	134	1.96(−6)	8.36	
02306+3420	0230+343	14,600	(242)	7.85 (0.05)	0.53 (0.00)	11.11	−2.08	16.0	95	1.63(−6)	8.23	
02386+3322	0238+333	13,390	(276)	8.23 (0.05)	0.75 (0.00)	11.82	−2.45	15.9	65	3.97(−6)	8.59	
02464+3239	0246+326	11,540	(173)	8.11 (0.05)	0.67 (0.00)	11.91	−2.64	15.8	59	4.46(−6)	8.68	
02503−0238	0250−026	14,740	(241)	7.87 (0.05)	0.54 (0.00)	11.12	−2.07	14.73	52	1.65(−6)	8.23	
03036−0043	0303−007	18,640	(413)	7.97 (0.07)	0.61 (0.00)	10.86	−1.72	16.21	117	1.20(−6)	7.94	1
03106−0719	0310−073	17,490	(323)	7.89 (0.06)	0.56 (0.00)	10.84	−1.78	16.7	148	1.17(−6)	7.97	

Table 3—Continued

KUV	WD	$T_{\rm eff}$	(K)	log g	$M/M_\odot$	M_V	log $L/L_\odot$	V	D(pc)	$1/v_{\rm max}$	log τ	Notes
03123+0155	0312+019	41,140	(854)	8.02 (0.08)	0.69 (0.00)	9.45	−0.34	17.5	406	—	6.57	
03184−0211	0318−021	12,800	(217)	7.93 (0.05)	0.57 (0.00)	11.47	−2.36	16.01	80	2.55(−6)	8.46	
03205−0005	0320−000	13,180	(499)	7.73 (0.07)	0.46 (0.00)	11.13	−2.19	16.97	147	1.67(−6)	8.30	
03217−0240	0321−026	26,890	(530)	8.46 (0.08)	0.92 (0.00)	10.96	−1.39	17.67	219	—	7.83	
03290+0053	0328+008	34,650	(564)	7.92 (0.07)	0.62 (0.00)	9.55	−0.58	16.8	282	2.61(−7)	6.79	
03292+0035	0329+005	15,500	(296)	8.00 (0.06)	0.61 (0.00)	11.22	−2.06	16.7	124	1.87(−6)	8.25	3
03295−0108	0329−011	17,070	(306)	7.76 (0.06)	0.49 (0.00)	10.70	−1.75	17.17	196	9.88(−7)	7.91	
03301−0100	0330−009	33,800	(510)	7.91 (0.05)	0.61 (0.00)	9.57	−0.61	15.86	181	2.66(−7)	6.82	
03302−0143	0330−017	30,290	(460)	7.86 (0.05)	0.58 (0.00)	9.72	−0.78	17.12	302	3.15(−7)	6.98	
03351+0245	0335+027	16,080	(289)	7.96 (0.05)	0.59 (0.00)	11.09	−1.97	17.4	182	1.59(−6)	8.17	
03363+0400	0336+040	8820	(129)	8.19 (0.06)	0.71 (0.00)	12.96	−3.16	15.9	38	1.74(−5)	9.04	
03383−0146	0338−017	20,500	(374)	8.18 (0.05)	0.73 (0.00)	11.00	−1.67	17.53	202	—	7.98	
03399+0015	0339+002A	13,680	(193)	7.97 (0.04)	0.59 (0.00)	11.39	−2.26	17.72	184	—	8.39	2
03416+0206	0341+021	22,310	(341)	7.46 (0.05)	0.39 (0.00)	9.77	−1.09	15.8	160	3.33(−7)	7.36	
03439−0048	0343−007	61,810	(1358)	7.84 (0.07)	0.65 (0.00)	8.66	+0.53	14.91	177	1.02(−7)	6.06	4
03442+0719	0344+073	10,930	(164)	7.84 (0.06)	0.51 (0.00)	11.67	−2.58	16.10	77	3.29(−6)	8.59	
03459+0037	0345+006	86,850	(3544)	7.08 (0.12)	0.51 (0.00)	6.49	+1.77	16.00	799	1.63(−8)	4.70	4, 5
03463−0108	0346−011	41,260	(765)	9.11 (0.07)	1.26 (0.00)	11.50	−1.15	14.06	32	2.65(−6)	7.93	
03521+0150	0352+018	22,350	(353)	7.92 (0.05)	0.59 (0.00)	10.46	−1.36	15.2	88	7.41(−7)	7.52	
03520+0500	0352+049	36,270	(592)	8.77 (0.06)	1.10 (0.00)	10.97	−1.10	16.2	111	1.37(−6)	7.78	
03520+0515	0352+052	10,280	(151)	8.10 (0.06)	0.66 (0.00)	12.25	−2.84	15.9	53	6.90(−6)	8.81	
03522+0737	0352+076	15,230	(278)	7.74 (0.06)	0.48 (0.00)	10.89	−1.94	16.76	149	1.25(−6)	8.09	
03526+0939	0352+096	14,030	(341)	8.19 (0.05)	0.73 (0.00)	11.68	−2.35	14.56	37	3.33(−6)	8.51	
03561+0807	0356+081	43,780	(840)	8.05 (0.07)	0.70 (0.00)	9.42	−0.24	16.7	286	2.26(−7)	6.50	
04100+1144	0410+117	20,630	(326)	7.95 (0.05)	0.60 (0.00)	10.65	−1.53	14.03	47	9.30(−7)	7.72	
04190+1522	0418+153	13,490	(346)	7.99 (0.05)	0.60 (0.00)	11.45	−2.30	16.62	107	2.49(−6)	8.43	
04211+1614	0421+162	19,140	(299)	8.05 (0.05)	0.65 (0.00)	10.92	−1.72	14.27	46	1.29(−6)	7.97	
04234+1222	0423+123	21,360	(497)	7.94 (0.07)	0.60 (0.00)	10.57	−1.46	16.9	184	8.45(−7)	7.64	
04239+1406	0423+140	12,820	(454)	8.89 (0.08)	1.15 (0.00)	13.05	−3.01	17.56	79	—	9.17	
04258+1652	0425+168	24,200	(371)	8.07 (0.05)	0.67 (0.00)	10.54	−1.32	13.92	47	8.15(−7)	7.51	

Table 3—Continued

KUV	WD	$T_{\rm eff}$	(K)	log g	$M/M_\odot$	M_V	log $L/L_\odot$	V	D(pc)	$1/v_{\rm max}$	log τ	Notes
04262+1038	0426+106	10,380	(154)	8.66 (0.05)	1.02 (0.00)	13.16	−3.19	16.3	42	2.27(−5)	9.26	
04295+1739	0429+176	17,540	(481)	7.98 (0.08)	0.61 (0.00)	10.97	−1.83	13.93	39	1.37(−6)	8.05	1
04304+1339	0430+136	35,720	(837)	8.11 (0.12)	0.72 (0.00)	9.80	−0.65	16.50	218	3.44(−7)	6.81	1
04310+1236	0431+126	20,810	(327)	8.09 (0.05)	0.68 (0.00)	10.84	−1.59	14.24	47	1.17(−6)	7.86	
04370+1514	0437+152	18,660	(322)	7.39 (0.05)	0.35 (0.00)	10.00	−1.36	15.83	146	4.33(−7)	7.50	
04383+1054	0438+108	26,820	(394)	8.08 (0.05)	0.68 (0.00)	10.33	−1.14	13.86	50	6.35(−7)	7.26	
06548+3225	0654+324	22,020	(386)	8.09 (0.05)	0.68 (0.00)	10.74	−1.50	18.1	295	—	7.75	
07069+2929	0706+294	14,040	(253)	7.84 (0.05)	0.52 (0.00)	11.17	−2.14	15.45	71	1.76(−6)	8.28	
07170+3653	0717+368	23,870	(470)	7.97 (0.06)	0.62 (0.00)	10.41	−1.28	16.8	190	6.99(−7)	7.42	
07540+4015	0754+402	18,830	(481)	7.89 (0.08)	0.56 (0.00)	10.72	−1.65	16.7	157	1.01(−6)	7.84	
08016+4206	0801+421	13,730	(560)	8.14 (0.07)	0.69 (0.00)	11.63	−2.35	17.06	121	3.12(−6)	8.50	
08026+4118	0802+413	51,890	(977)	7.60 (0.06)	0.53 (0.00)	8.43	+0.38	14.5	163	8.14(−8)	6.27	
08039+4003	0803+400	12,450	(247)	8.07 (0.06)	0.65 (0.00)	11.71	−2.48	17.40	137	3.46(−6)	8.57	
08084+4221	0808+423	14,900	(446)	8.90 (0.05)	1.15 (0.00)	12.81	−2.75	16.76	61	1.43(−5)	9.00	
08100+3915	0810+392	22,540	(453)	7.91 (0.06)	0.58 (0.00)	10.42	−1.34	16.85	193	7.07(−7)	7.48	
08157+3739	0815+376	21,690	(365)	7.95 (0.05)	0.60 (0.00)	10.55	−1.43	16.7	170	8.25(−7)	7.61	
08157+3946	0815+397	37,820	(727)	7.85 (0.08)	0.59 (0.00)	9.29	−0.37	17.40	419	1.96(−7)	6.65	
08165+3741	0816+376	11,000	(627)	8.00 (0.06)	0.60 (0.00)	11.88	−2.66	15.6	55	4.29(−6)	8.67	6
08167+3844	0816+387	7630	(112)	7.98 (0.07)	0.58 (0.00)	13.22	−3.29	16.55	46	2.46(−5)	9.07	
08172+3838	0817+386	25,330	(388)	8.03 (0.05)	0.65 (0.00)	10.38	−1.21	15.69	115	6.74(−7)	7.35	
08268+4150	0826+418	10,270	(158)	8.12 (0.07)	0.67 (0.00)	12.28	−2.85	16.8	80	7.17(−6)	8.82	
08275+3252	0827+328	7490	(115)	8.63 (0.08)	1.00 (0.00)	14.32	−3.74	15.73	19	—	9.56	
08273+4101	0827+410	15,210	(254)	7.77 (0.05)	0.49 (0.00)	10.93	−1.96	15.92	99	1.31(−6)	8.12	
08308+3710	0830+371	9180	(133)	8.26 (0.06)	0.76 (0.00)	12.92	−3.13	16.01	41	1.65(−5)	9.04	
08317+4117	0831+412	31,300	(510)	8.43 (0.07)	0.90 (0.00)	10.57	−1.10	17.11	202	8.45(−7)	7.54	
08354+3639	0835+366	15,690	(284)	7.91 (0.05)	0.56 (0.00)	11.07	−1.98	17.87	229	—	8.17	
08368+4026	0836+404	11,870	(180)	8.10 (0.05)	0.67 (0.00)	11.84	−2.59	15.55	55	4.08(−6)	8.65	
08371+3754	0837+378	14,340	(440)	8.17 (0.06)	0.71 (0.00)	11.61	−2.30	17.50	150	—	8.47	
08378+3934	0837+395	20,420	(485)	7.89 (0.07)	0.56 (0.00)	10.57	−1.50	16.54	156	8.45(−7)	7.67	
08381+3737	0838+376	19,040	(328)	7.88 (0.05)	0.56 (0.00)	10.68	−1.62	16.99	182	9.65(−7)	7.80	

Table 3—Continued

KUV	WD	$T_{\rm eff}$	(K)	log g	$M/M_\odot$	M_V	log $L/L_\odot$	V	D(pc)	$1/v_{\rm max}$	log τ	Notes
08397+3435	0839+345	17,550	(286)	8.06 (0.05)	0.65 (0.00)	11.08	−1.87	16.2	105	1.57(−6)	8.11	
08391+3800	0839+379	19,020	(376)	8.06 (0.06)	0.65 (0.00)	10.94	−1.73	16.32	119	1.32(−6)	7.99	
08411+3340	0841+336	23,990	(461)	8.12 (0.06)	0.70 (0.00)	10.63	−1.36	16.7	163	9.08(−7)	7.60	
08417+4112	0841+411	16,070	(336)	7.92 (0.06)	0.57 (0.00)	11.04	−1.95	17.40	187	1.50(−6)	8.14	
08422+3813	0842+382	7990	(116)	8.06 (0.06)	0.63 (0.00)	13.15	−3.26	16.03	37	2.24(−5)	9.07	4
08460+3441	0846+346	7600	(110)	8.07 (0.06)	0.63 (0.00)	13.36	−3.35	15.72	29	2.95(−5)	9.13	
08473+3838	0847+386	17,280	(286)	8.30 (0.05)	0.80 (0.00)	11.48	−2.05	17.67	172	—	8.32	
08504+4155	0850+419	18,200	(321)	7.87 (0.05)	0.55 (0.00)	10.75	−1.70	16.9	169	1.05(−6)	7.89	
08543+4028	0854+404	22,270	(341)	7.93 (0.05)	0.59 (0.00)	10.47	−1.37	14.90	76	7.50(−7)	7.53	
08587+3619	0858+363	11,970	(178)	8.17 (0.05)	0.71 (0.00)	11.93	−2.62	14.55	33	4.57(−6)	8.68	
09029+4153	0902+418	44,040	(1029)	8.05 (0.09)	0.71 (0.00)	9.42	−0.23	17.2	360	2.26(−7)	6.49	
09272+3930	0927+394	23,940	(486)	8.32 (0.07)	0.82 (0.00)	10.95	−1.49	17.7	224	—	7.87	
09288+3959	0928+399	25,300	(503)	8.04 (0.07)	0.66 (0.00)	10.40	−1.22	17.53	267	—	7.36	
09443+4229	0944+424	23,680	(368)	8.02 (0.05)	0.64 (0.00)	10.49	−1.32	16.43	154	7.68(−7)	7.49	
09479+3234	0947+325	22,200	(345)	8.31 (0.05)	0.81 (0.00)	11.07	−1.62	15.38	72	1.55(−6)	7.98	
09538+3405	0953+340	16,640	(395)	8.01 (0.07)	0.62 (0.00)	11.11	−1.94	16.76	134	1.63(−6)	8.16	
09583+3520	0958+353	40,940	(897)	7.93 (0.09)	0.64 (0.00)	9.31	−0.28	16.9	330	2.00(−7)	6.56	
10010+3318	1001+333	9760	(143)	8.21 (0.06)	0.73 (0.00)	12.61	−3.00	16.3	54	1.10(−5)	8.94	
10013+3614	1001+362	9450	(142)	7.33 (0.09)	0.30 (0.00)	11.47	−2.57	16.8	116	2.55(−6)	8.56	
10063+3522	1006+353	19,920	(461)	7.85 (0.07)	0.55 (0.00)	10.56	−1.53	17.83	283	—	7.68	
10090+3712	1008+372	15,150	(272)	7.91 (0.05)	0.56 (0.00)	11.12	−2.04	16.8	136	1.65(−6)	8.21	
10081+3817	1008+382	13,160	(356)	7.87 (0.06)	0.54 (0.00)	11.33	−2.27	16.29	98	2.14(−6)	8.38	
10115+3332	1011+335	19,690	(404)	8.11 (0.06)	0.69 (0.00)	10.97	−1.71	17.4	193	1.37(−6)	7.98	
11230+4240	1123+426	10,400	(156)	8.18 (0.06)	0.71 (0.00)	12.33	−2.87	17.0	86	7.65(−6)	8.85	
11265+3825	1126+384	25,060	(388)	7.96 (0.05)	0.61 (0.00)	10.30	−1.18	14.89	82	6.13(−7)	7.30	
11370+4222	1137+423	11,840	(178)	8.15 (0.05)	0.70 (0.00)	11.92	−2.62	16.56	84	4.52(−6)	8.68	
11390+4225	1139+424	27,250	(425)	7.90 (0.05)	0.59 (0.00)	10.02	−1.00	16.20	172	4.43(−7)	7.10	
11472+3858	1147+389	17,220	(311)	7.89 (0.05)	0.56 (0.00)	10.87	−1.81	17.46	207	—	8.00	
11491+4104	1149+410	14,070	(271)	7.84 (0.05)	0.52 (0.00)	11.17	−2.14	16.08	96	1.76(−6)	8.28	
12279+3044	1227+307	13,330	(544)	7.93 (0.07)	0.57 (0.00)	11.39	−2.28	17.7	182	—	8.40	

Table 3—Continued

KUV	WD	$T_{\rm eff}$	(K)	log g	$M/M_\odot$	M_V	log $L/L_\odot$	V	D(pc)	$1/v_{\rm max}$	log τ	Notes
12353+2925	1235+294	18,850	(357)	7.90 (0.06)	0.56 (0.00)	10.72	−1.65	17.29	205	1.01(−6)	7.84	
12399+2744	1239+277	14,740	(256)	7.84 (0.05)	0.52 (0.00)	11.08	−2.06	15.7	83	1.57(−6)	8.21	
12420+2938	1241+296	17,870	(354)	7.81 (0.06)	0.52 (0.00)	10.70	−1.70	16.0	114	9.88(−7)	7.87	
12436+3011	1243+301	14,140	(369)	7.75 (0.07)	0.48 (0.00)	11.03	−2.08	17.60	206	—	8.21	
12474+3105	1247+310	11,940	(216)	8.34 (0.06)	0.82 (0.00)	12.19	−2.72	17.2	100	6.38(−6)	8.80	
12492+2937	1249+296	11,770	(211)	8.25 (0.06)	0.76 (0.00)	12.09	−2.69	16.8	87	5.61(−6)	8.76	
12574+2750	1257+278	8710	(126)	8.36 (0.06)	0.82 (0.00)	13.28	−3.29	15.39	26	2.66(−5)	9.19	
12587+2942	1258+297	14,830	(306)	7.91 (0.06)	0.56 (0.00)	11.16	−2.08	18.3	267	—	8.25	
13088+3139	1308+316	13,260	(444)	7.93 (0.06)	0.57 (0.00)	11.40	−2.29	16.79	119	2.34(−6)	8.41	
14083+3223	1408+323	18,160	(279)	7.91 (0.05)	0.57 (0.00)	10.81	−1.73	14.11	45	1.13(−6)	7.93	
14134+2311	1413+231	23,290	(412)	7.74 (0.05)	0.50 (0.00)	10.10	−1.18	16.9	228	4.86(−7)	7.33	
14138+2408	1413+241	16,450	(265)	8.05 (0.05)	0.65 (0.00)	11.19	−1.98	17.0	145	1.80(−6)	8.20	
14197+2514	1419+252A	10,160	(143)	8.00 (0.04)	0.60 (0.00)	12.14	−2.80	18.10	155	—	8.76	2
14205+2251	1420+228	17,300	(319)	7.83 (0.06)	0.52 (0.00)	10.78	−1.76	16.8	160	1.09(−6)	7.94	
14227+3340	1422+336	13,740	(430)	8.15 (0.06)	0.70 (0.00)	11.66	−2.36	17.1	122	3.24(−6)	8.51	
14287+3724	1428+373	14,010	(221)	7.36 (0.05)	0.32 (0.00)	10.50	−1.87	15.6	104	7.77(−7)	8.07	
14299+3720	1429+373	34,390	(507)	8.11 (0.05)	0.72 (0.00)	9.86	−0.71	15.27	120	3.69(−7)	6.88	
14310+2542	1431+257	22,610	(399)	7.21 (0.05)	0.32 (0.00)	9.32	−0.89	17.0	342	2.03(−7)	7.29	
15502+1819	1550+183	14,260	(271)	8.25 (0.05)	0.77 (0.00)	11.75	−2.36	14.9	42	3.64(−6)	8.53	
16055+1745	1605+177	13,830	(267)	7.68 (0.05)	0.44 (0.00)	10.97	−2.07	16.7	140	1.37(−6)	8.20	
16069+1810	1606+181	22,150	(373)	7.98 (0.05)	0.62 (0.00)	10.56	−1.42	17.1	202	8.35(−7)	7.60	
16075+2031	1607+205	11,150	(173)	7.82 (0.06)	0.50 (0.00)	11.58	−2.53	17.4	145	2.93(−6)	8.56	
16106+3820	1610+383	14,450	(278)	7.83 (0.05)	0.52 (0.00)	11.10	−2.08	16.4	114	1.61(−6)	8.23	
16195+4125	1619+414	14,090	(457)	7.93 (0.06)	0.57 (0.00)	11.28	−2.18	16.8	126	2.01(−6)	8.33	1
16268+4055	1626+409	21,400	(422)	7.98 (0.06)	0.62 (0.00)	10.63	−1.48	16.7	163	9.08(−7)	7.68	
16288+3904	1628+390	19,040	(340)	7.88 (0.05)	0.56 (0.00)	10.68	−1.62	16.8	167	9.65(−7)	7.80	
16319+3937	1631+396	17,380	(281)	7.63 (0.05)	0.43 (0.00)	10.49	−1.64	14.1	52	7.68(−7)	7.80	
16366+3506	1636+351	36,950	(561)	8.04 (0.05)	0.69 (0.00)	9.63	−0.54	14.9	113	2.85(−7)	6.73	
16376+3331	1637+335	10,260	(147)	8.20 (0.05)	0.72 (0.00)	12.41	−2.90	14.8	30	8.49(−6)	8.88	
16476+3733	1647+375	21,860	(343)	7.92 (0.05)	0.59 (0.00)	10.50	−1.40	14.98	78	7.77(−7)	7.57	

Table 3—Continued

KUV	WD	$T_{\rm eff}$	(K)	log g	$M/M_\odot$	M_V	log $L/L_\odot$	V	D(pc)	$1/v_{\rm max}$	log τ	Notes
16484+3706	1648+371	42,240	(904)	7.63 (0.08)	0.51 (0.00)	8.75	−0.02	15.91	270	1.12(−7)	6.53	
18004+6836	1800+685	44,110	(783)	7.90 (0.06)	0.63 (0.00)	9.16	−0.13	14.60	122	1.71(−7)	6.47	4
18284+6650	1828+668	10,800	(163)	8.20 (0.06)	0.73 (0.00)	12.24	−2.81	16.65	76	6.81(−6)	8.82	
18332+6429	1833+644	46,300	(1764)	8.12 (0.14)	0.75 (0.00)	9.48	−0.19	16.9	304	2.41(−7)	6.42	1
18453+6819	1845+683	36,810	(574)	8.31 (0.05)	0.84 (0.00)	10.08	−0.73	15.00	96	4.75(−7)	6.88	4
21168+7338	2116+736	52,810	(1182)	7.66 (0.08)	0.56 (0.00)	8.52	+0.37	14.87	186	8.88(−8)	6.27	
21267+7326	2126+734	15,290	(223)	7.84 (0.04)	0.53 (0.00)	11.02	−1.99	12.78	22	1.46(−6)	8.16	
22543+1237	2254+126	11,640	(173)	8.05 (0.05)	0.64 (0.00)	11.81	−2.59	16.0	68	3.92(−6)	8.64	
22570+1349	2257+138	27,300	(399)	8.36 (0.05)	0.85 (0.00)	10.74	−1.29	16.65	151	1.04(−6)	7.66	
22573+1613	2257+162	24,840	(386)	7.49 (0.05)	0.41 (0.00)	9.60	−0.91	16.14	203	2.75(−7)	7.23	
23060+1303	2306+124	20,340	(322)	8.06 (0.05)	0.66 (0.00)	10.84	−1.62	15.23	75	1.17(−6)	7.88	
23061+1229	2306+130	13,250	(283)	7.92 (0.05)	0.56 (0.00)	11.38	−2.29	15.1	55	2.28(−6)	8.40	
23083+1642	2308+167	18,000	(322)	7.95 (0.05)	0.59 (0.00)	10.88	−1.76	17.2	184	1.23(−6)	7.97	
23098+1031	2309+105	54,150	(951)	8.00 (0.06)	0.70 (0.00)	9.09	+0.17	13.09	63	1.59(−7)	6.20	
23128+1157	2312+119	18,100	(306)	7.70 (0.05)	0.46 (0.00)	10.51	−1.61	17.83	291	—	7.76	
23149+1408	2314+141	17,840	(304)	7.78 (0.05)	0.50 (0.00)	10.65	−1.68	16.9	177	9.30(−7)	7.85	
23162+1220	2316+123	11,000	(383)	8.00 (0.06)	0.60 (0.00)	11.88	−2.66	15.38	50	4.29(−6)	8.67	7
23176+2650	2317+268	31,480	(491)	7.68 (0.06)	0.50 (0.00)	9.34	−0.59	16.3	246	2.07(−7)	6.91	
23189+0901	2318+090	28,990	(475)	7.97 (0.06)	0.63 (0.00)	10.00	−0.93	16.27	179	4.33(−7)	7.02	
23180+1242	2318+126	13,490	(334)	7.92 (0.05)	0.56 (0.00)	11.35	−2.25	16.27	96	2.20(−6)	8.38	
23220+0921	2322+093	14,060	(304)	7.81 (0.06)	0.51 (0.00)	11.12	−2.12	16.7	130	1.65(−6)	8.26	
23223+0953	2322+098	20,090	(341)	7.88 (0.05)	0.56 (0.00)	10.59	−1.53	17.2	210	8.66(−7)	7.69	
23235+2536	2323+256	5930	(279)	7.85 (0.66)	0.50 (0.00)	14.11	−3.67	17.02	38	—	9.27	
23282+1046	2328+107	22,180	(363)	7.85 (0.05)	0.55 (0.00)	10.37	−1.34	15.53	107	6.66(−7)	7.48	
23296+2642	2329+267	9400	(274)	8.02 (0.28)	0.61 (0.00)	12.46	−2.95	15.4	38	9.06(−6)	8.86	8

Note. — (1) DA+dM; (2) Unresolved double degenerate; (3) Magnetic, $B = 12$ MG (Jordan 1993), $T_{\rm eff}$ from Schmidt et al. 2003; (4) Not in Darling 1994; (5) DAO star; (6) Magnetic, $B = 9$ MG (Angel et al. (1974), $T_{\rm eff}$ from Jordan 2001; (7) Magnetic, $B = 29$ MG and $T_{\rm eff}$ from Liebert et al. (1985); (8) Magnetic, B (2.3 MG), $T_{\rm eff}$ and $\log g$ from Bergeron et al. 2001.

Table 4. Atmospheric Parameters of DB Stars from the KUV Sample

KUV	WD	$T_{\rm eff}$	(K)	log g	log H/He	$M/M_\odot$	M_V	log $L/L_\odot$	V	D(pc)	$1/v_{\rm max}$	log τ	Notes
00312−1837	0031−186	15,270	(249)	8.43 (0.09)	—	0.86 (0.00)	11.93	−2.36	16.66	88	4.64(−6)	8.59	
01254−2340	0125−236	16,500	(261)	8.29 (0.08)	−4.80	0.77 (0.00)	11.53	−2.14	15.38	58	2.79(−6)	8.39	
02196+2816	0219+282B	36,340	(512)	8.09 (0.04)	—	0.68 (0.00)	10.11	−0.62	17.90	361	—	6.96	1
02499+3442	0249+346	13,440	(350)	9.02 (0.18)	−4.64	1.20 (0.00)	13.35	−3.04	16.40	40	2.96(−5)	9.14	
02498−0515	0249−052	17,400	(265)	8.05 (0.06)	—	0.62 (0.00)	11.03	−1.90	16.60	129	1.50(−6)	8.15	
03003−0120	0300−013	14,280	(298)	7.91 (0.18)	—	0.54 (0.00)	11.30	−2.17	15.56	71	2.09(−6)	8.32	
03399+0015	0339+002B	13,730	(194)	8.00 (0.04)	—	0.59 (0.00)	11.57	−2.29	17.82	177	—	8.44	1
03493+0131	0349+015	25,300	(700)	7.98 (0.05)	—	0.60 (0.00)	10.42	−1.20	17.2	226	7.16(−7)	7.37	
04376+1353	0437+138	15,330	(239)	8.36 (0.08)	−4.55	0.82 (0.00)	11.82	−2.32	14.92	41	4.03(−6)	8.54	
05034+1445	0503+147	15,460	(229)	8.03 (0.07)	−4.86	0.61 (0.00)	11.28	−2.10	13.08	22	2.04(−6)	8.31	
05134+2605	0513+260	26,170	(549)	8.24 (0.05)	—	0.75 (0.00)	10.77	−1.30	16.70	153	1.09(−6)	7.57	
08381+3737	0838+375	13,640	(390)	8.24 (0.25)	—	0.73 (0.00)	11.88	−2.44	17.	105	4.35(−6)	8.59	
10064+4120	1006+413	15,170	(358)	8.86 (0.18)	−5.09	1.12 (0.00)	12.75	−2.69	17.83	103	—	8.95	
10098+4138	1009+416	16,430	(258)	8.69 (0.08)	−4.83	1.02 (0.00)	12.24	−2.42	16.33	65	6.91(−6)	8.68	
11489+4052	1148+408	17,230	(321)	8.39 (0.11)	−4.48	0.84 (0.00)	11.60	−2.13	17.33	139	3.05(−6)	8.42	
14156+2325	1415+234	17,590	(270)	8.17 (0.06)	—	0.70 (0.00)	11.20	−1.95	16.8	132	1.85(−6)	8.22	
14161+2255	1416+229	17,590	(276)	8.18 (0.07)	—	0.70 (0.00)	11.21	−1.96	16.9	119	1.87(−6)	8.22	1
14197+2514	1419+252B	14,520	(205)	8.00 (0.04)	—	0.59 (0.00)	11.44	−2.19	17.34	151	2.49(−6)	8.37	1
14200+3509	1419+351	12,770	(547)	8.85 (0.35)	−4.57	1.12 (0.00)	13.12	−2.99	16.0	37	2.18(−5)	9.14	
15519+1730	1551+175	15,440	(268)	7.89 (0.13)	−4.34	0.53 (0.00)	11.09	−2.02	17.5	191	—	8.19	
15571+1913	1557+192	19,380	(375)	8.17 (0.06)	−3.78	0.70 (0.00)	11.00	−1.78	15.4	75	1.44(−6)	8.07	
16454+3234	1645+325	25,170	(472)	7.94 (0.05)	—	0.58 (0.00)	10.37	−1.18	14.0	53	6.75(−7)	7.35	
23103+1736	2310+175	15,170	(270)	8.29 (0.15)	−6.49	0.77 (0.00)	11.73	−2.29	15.88	67	3.59(−6)	8.50	

Note. — (1) Unresolved double degenerate.

Fig. 1.— Optical spectra of hot subdwarfs or main sequence stars misclassified as DA or DB stars in the Kiso survey (Darling 1994, and references therein). The objects are approximately ordered as a function of their slope. KUV 16032+1735 (left panel, fourth object from the top) is a hot sdO star.

Fig. 2.— Optical spectra for a subsample of DA white dwarfs from the Kiso survey. The spectra are normalized at 4500 Å and are shifted vertically for clarity; the various zero points are indicated by long tick marks. The effective temperature decreases from upper left to bottom right. The hottest object in this sample is the DAO star KUV 03459+0037 displayed at the top of the left panel.

Fig. 3.— Same as Figure 2 but for a subsample of DO/DB(Z)/DBA(Z) white dwarfs from the Kiso survey. The hottest object in this sample is the DO star KUV 01018−1818 shown at the top.

Fig. 4.— Same as Figure 2 but for the magnetic white dwarfs in the Kiso survey; these all have hydrogen-rich atmospheres. The strength of the magnetic field increases from top ($B \sim 2.3$ MG) to bottom ($B \sim 29$ MG, see references in Table 3).

Fig. 5.— Our best fits to the optical spectra of the three DAB stars in our sample with composite DA+DB models. The atmospheric parameters for each solution are given in the figure. Both the observed and theoretical spectra are normalized to a continuum set to unity and the spectra are shifted from each other for clarity. The detailed analysis of KUV 02196+2816 has already been published in Limoges et al. (2009) while the details for KUV 03399+0015 and KUV 14197+2514 will be presented elsewhere.

Fig. 6.— Masses of all DA (*open circles*) and DB (*filled circles*) stars in the Kiso survey as a function of effective temperature, together with theoretical isochrones labeled in units of $\log \tau$, where τ is the white dwarf cooling age in years.

Fig. 7.— Our best fits to two DB stars near 15,000 K, but with significantly different values of $\log g$ (given in the figure). The spectra are normalized to a continuum set to unity and the best fitting models are shown as a thick line. The tick marks indicate the location of the He I λ3820 and λ4388 lines, which are the most gravity sensitive in this range of temperature.

Fig. 8.— Mass distributions for the 136 DA stars in the KUV sample with $T_{\rm eff} > 13,000$ K and the 23 DB white dwarfs. The masses of DA stars below this value may be biased, as explained in the text. Mean values and standard deviations of both distributions are given in the figure.

Fig. 9.— Comparison of luminosity functions of white dwarf stars from the Kiso survey, all spectral types included. The open circles represent the results published in Table 4.5 of Darling (1994), while the filled circles correspond to our attempt at reproducing his results using the same input data and method of calculation.

Fig. 10.— Comparison of the absolute visual magnitudes obtained from the empirical photometric calibration of Darling (1994) and from the spectroscopic method, for all DA and DB stars in common.

Fig. 11.— Luminosity functions for the DA and DB stars in the Kiso survey that are in common between our sample and that of Darling (1994). The open circles correspond to the luminosity function calculated using the approximate M_V values provided in Table 4.3 of Darling (1994), while the filled circles make use of the spectroscopic M_V values given in our Tables 3 and 4. The magnitude bin at 14.0 in Darling's data is empty since all cool DQ, DZ, and DC stars are excluded in this comparison. Also, the last two bins in our spectroscopic determination contain only one star each, and the corresponding error bars are too large and not shown here.

Fig. 12.— Comparison of the luminosity functions for DA white dwarfs in the Kiso survey (149 stars; this work) and in the PG survey (348 stars; LBH05).

Fig. 13.— The luminosity function for the complete sample of 168 white dwarfs (149 DA and 19 DB stars) found in the Kiso survey and based on our spectroscopic M_V values.

Fig. 14.— Our luminosity function for the complete sample of white dwarfs found in the Kiso survey plotted as a function of $M_{\rm bol}$ and compared to the luminosity functions obtained by Harris et al. (2006) and DeGennaro et al. (2008) for white dwarfs in the SDSS; the corresponding uncertainties are roughly equal to the size of the symbols used here and are thus not shown.

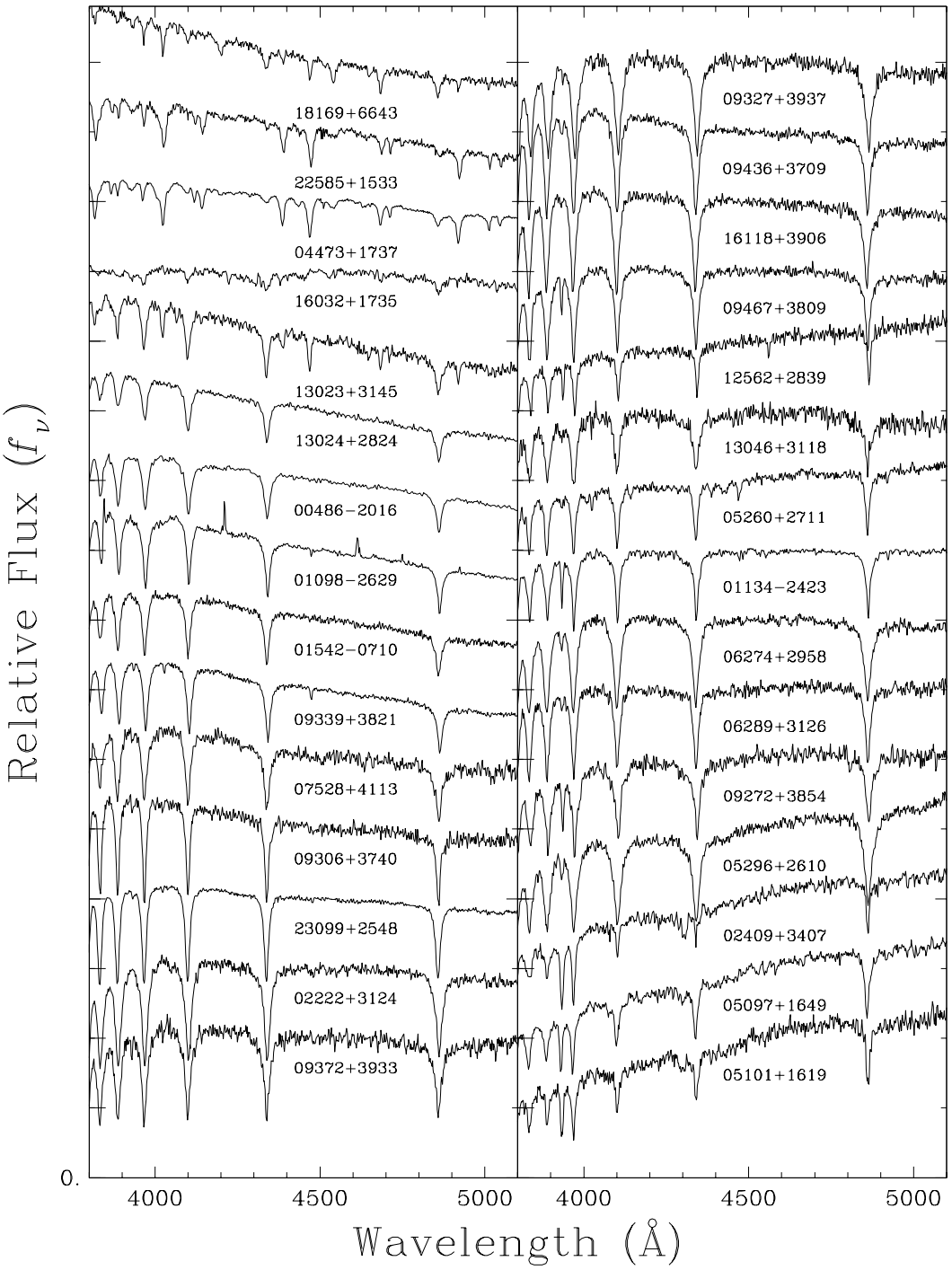
Relative Flux (f_ν)
0.
18169+6643
22585+1533
04473+1737
16032+1735
13023+3145
13024+2824
00486−2016
01098−2629
01542−0710
09339+3821
07528+4113
09306+3740
23099+2548
02222+3124
09372+3933
09327+3937
09436+3709
16118+3906
09467+3809
12562+2839
13046+3118
05260+2711
01134−2423
06274+2958
06289+3126
09272+3854
05296+2610
02409+3407
05097+1649
05101+1619
4000
4500
5000
4000
4500
5000
Wavelength (Å)

Figure 1

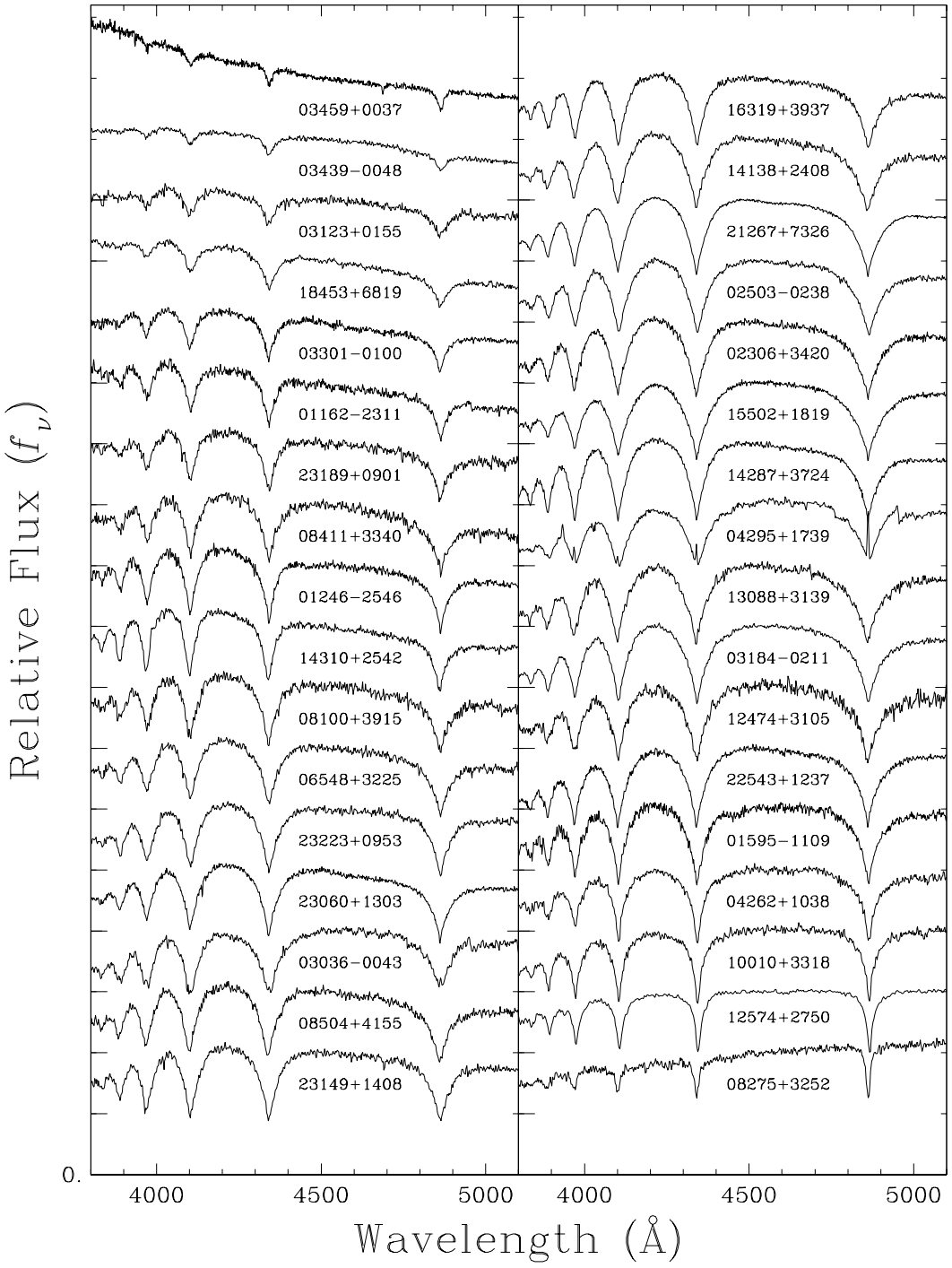
03459+0037
03439−0048
03123+0155
18453+6819
03301−0100
01162−2311
23189+0901
08411+3340
01246−2546
14310+2542
08100+3915
06548+3225
23223+0953
23060+1303
03036−0043
08504+4155
23149+1408
16319+3937
14138+2408
21267+7326
02503−0238
02306+3420
15502+1819
14287+3724
04295+1739
13088+3139
03184−0211
12474+3105
22543+1237
01595−1109
04262+1038
10010+3318
12574+2750
08275+3252
0.
4000
4500
5000
4000
4500
5000
Relative Flux (f_ν)
Wavelength (Å)

Figure 2

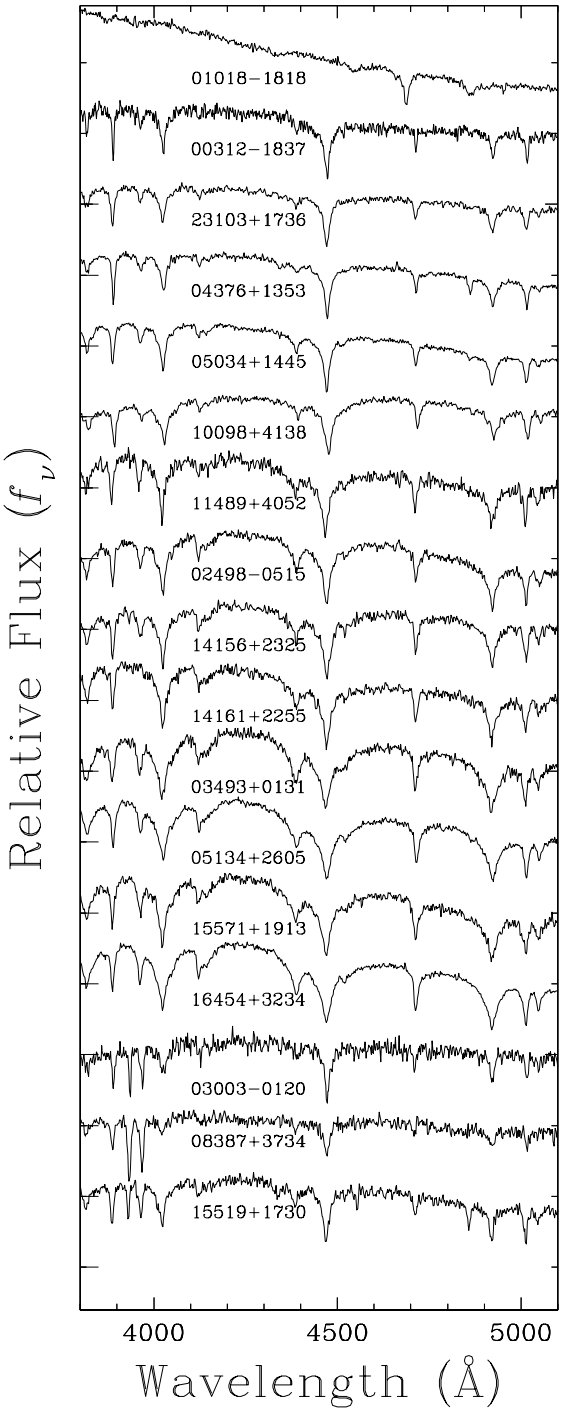
01018−1818
00312−1837
23103+1736
04376+1353
05034+1445
10098+4138
11489+4052
02498−0515
14156+2325
14161+2255
03493+0131
05134+2605
15571+1913
16454+3234
03003−0120
08387+3734
15519+1730
Relative Flux (f_ν)
4000
4500
5000
Wavelength (Å)

Figure 3

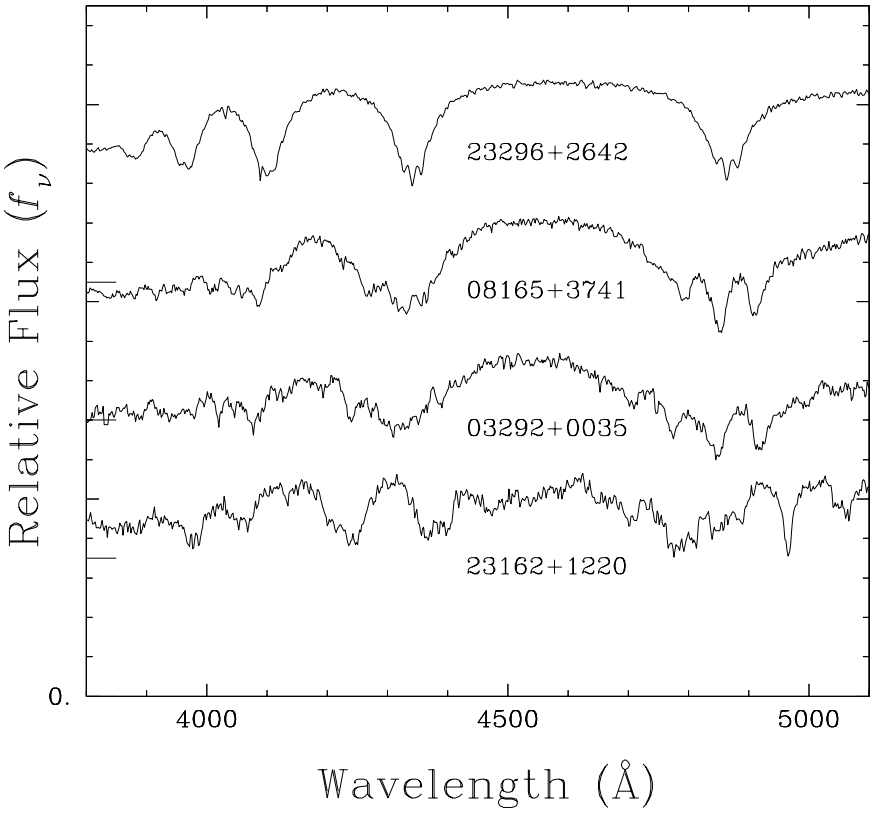
23296+2642
08165+3741
03292+0035
23162+1220
Relative Flux (f_ν)
0.
4000
4500
5000
Wavelength (Å)

Figure 4

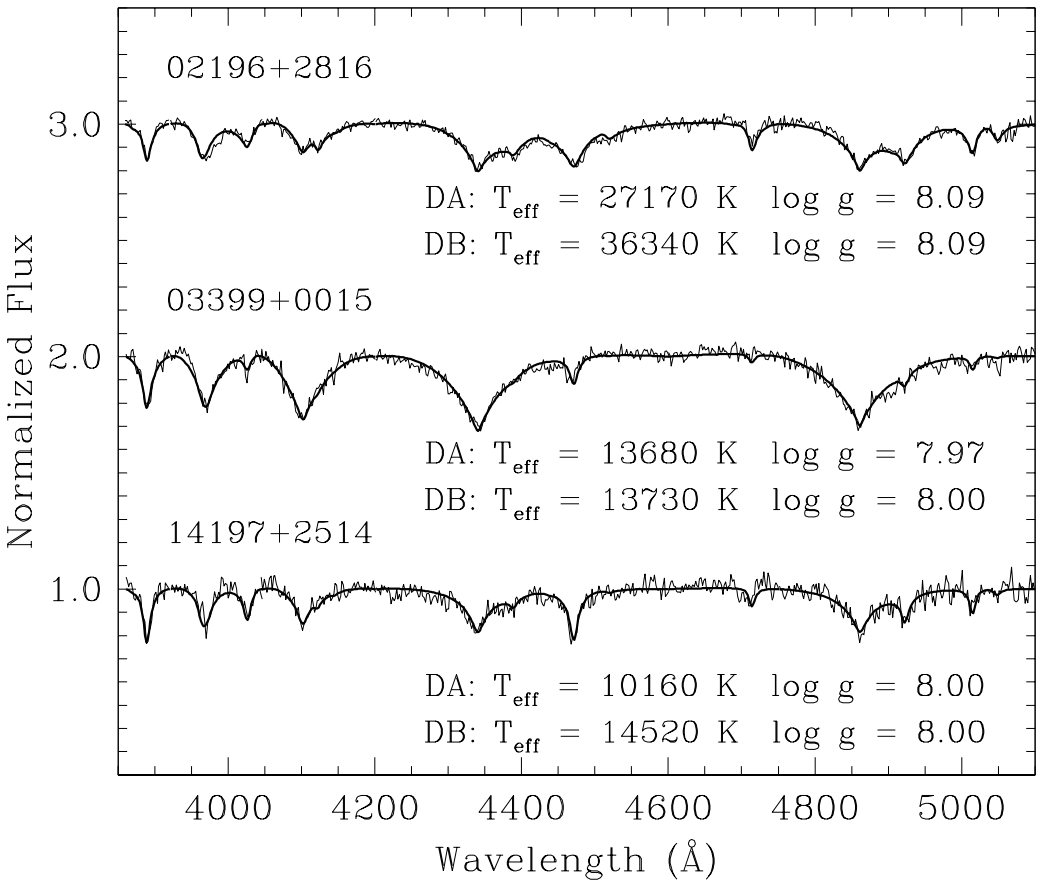
02196+2816
DA: T_eff = 27170 K log g = 8.09
DB: T_eff = 36340 K log g = 8.09
03399+0015
DA: T_eff = 13680 K log g = 7.97
DB: T_eff = 13730 K log g = 8.00
14197+2514
DA: T_eff = 10160 K log g = 8.00
DB: T_eff = 14520 K log g = 8.00
Normalized Flux
3.0
2.0
1.0
4000
4200
4400
4600
4800
5000
Wavelength (Å)

Figure 5

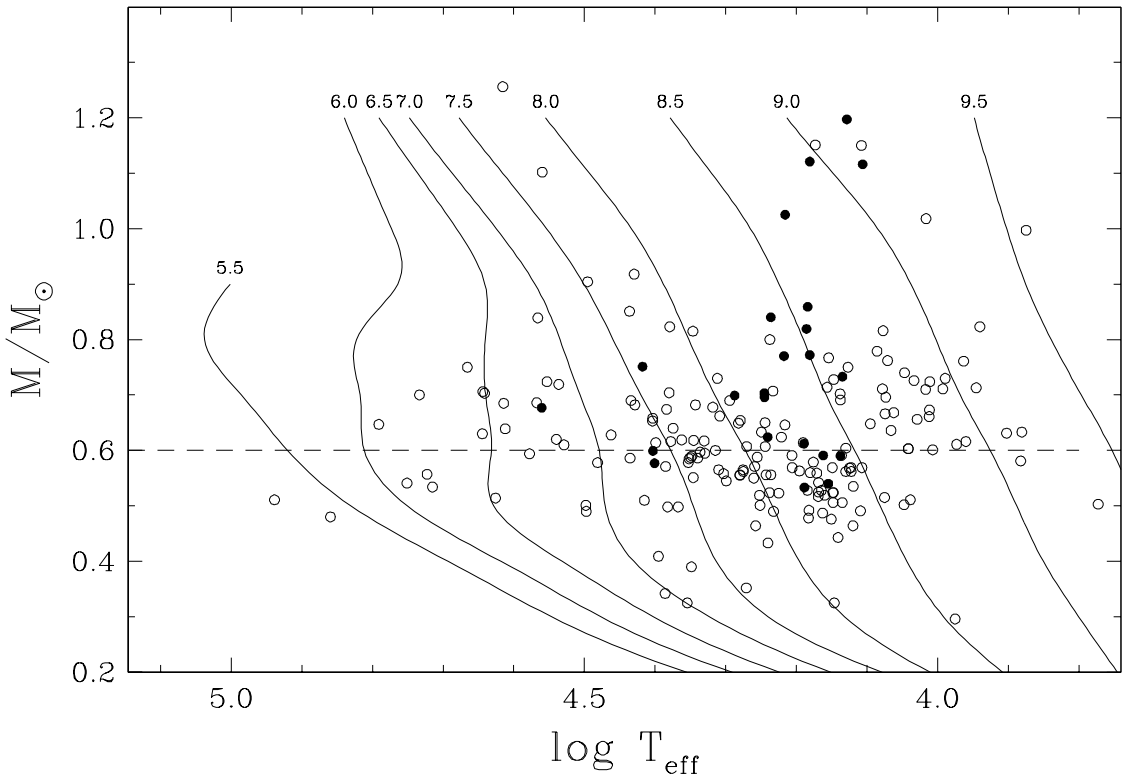

Figure 6

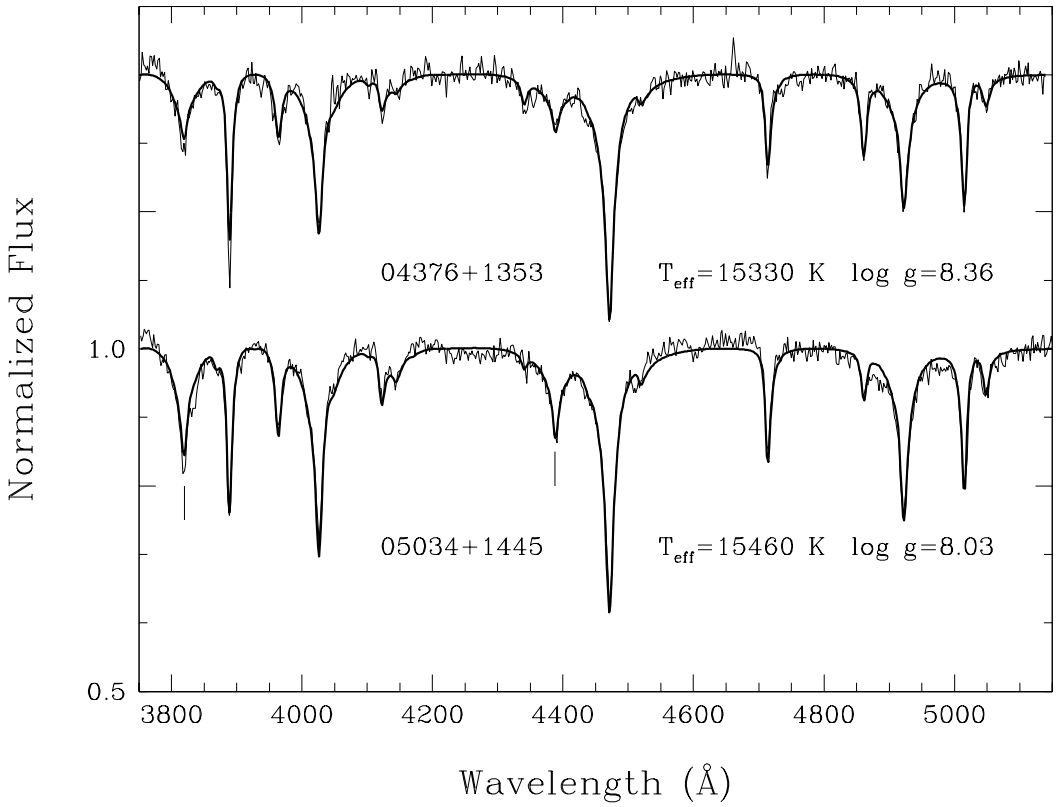
Normalized Flux
1.0
0.5
04376+1353
T_eff=15330 K log g=8.36
05034+1445
T_eff=15460 K log g=8.03
3800
4000
4200
4400
4600
4800
5000
Wavelength (Å)

Figure 7

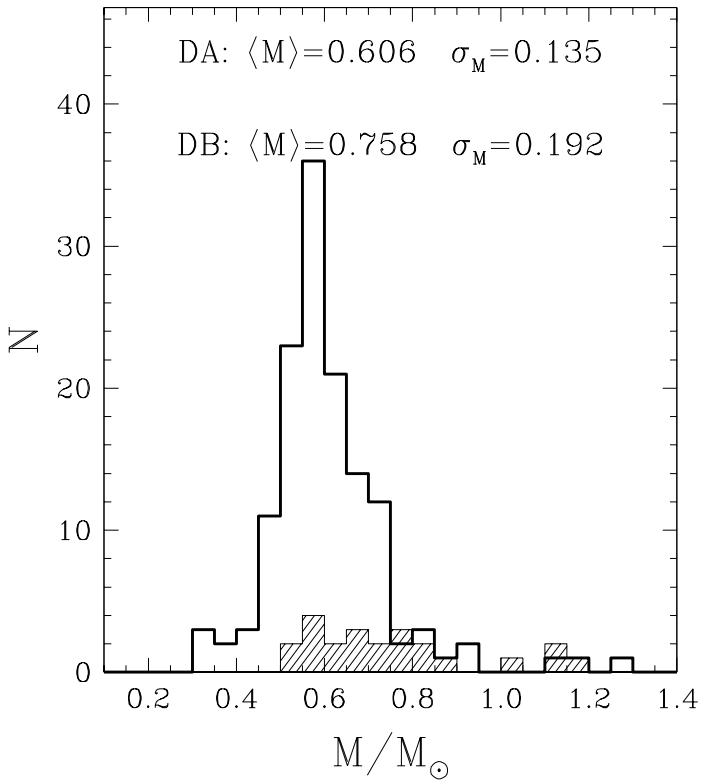
DA: ⟨M⟩=0.606 σ_M=0.135
DB: ⟨M⟩=0.758 σ_M=0.192
N
M/M_⊙
0
10
20
30
40
0.2
0.4
0.6
0.8
1.0
1.2
1.4

Figure 8

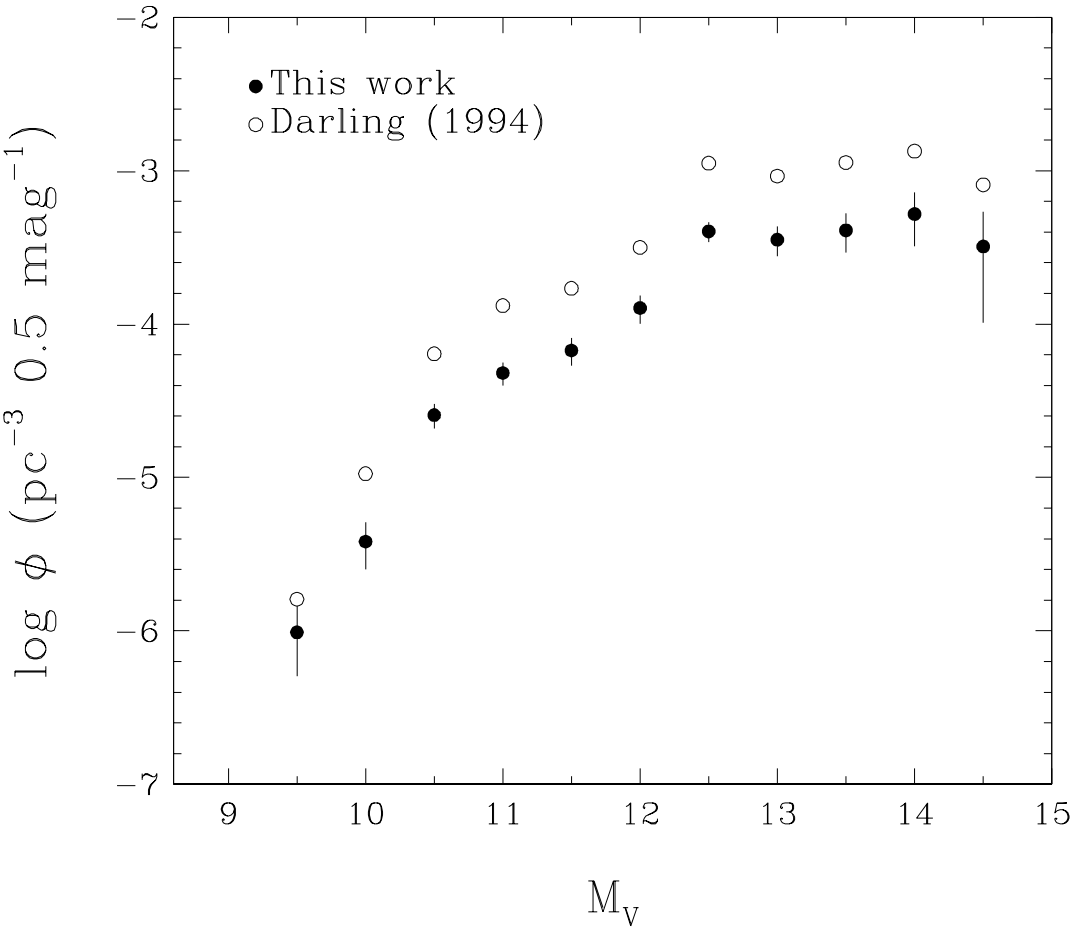
This work
Darling (1994)
log φ (pc^{-3} 0.5 mag^{-1})
M$_V$
−2
−3
−4
−5
−6
−7
9
10
11
12
13
14
15

Figure 9

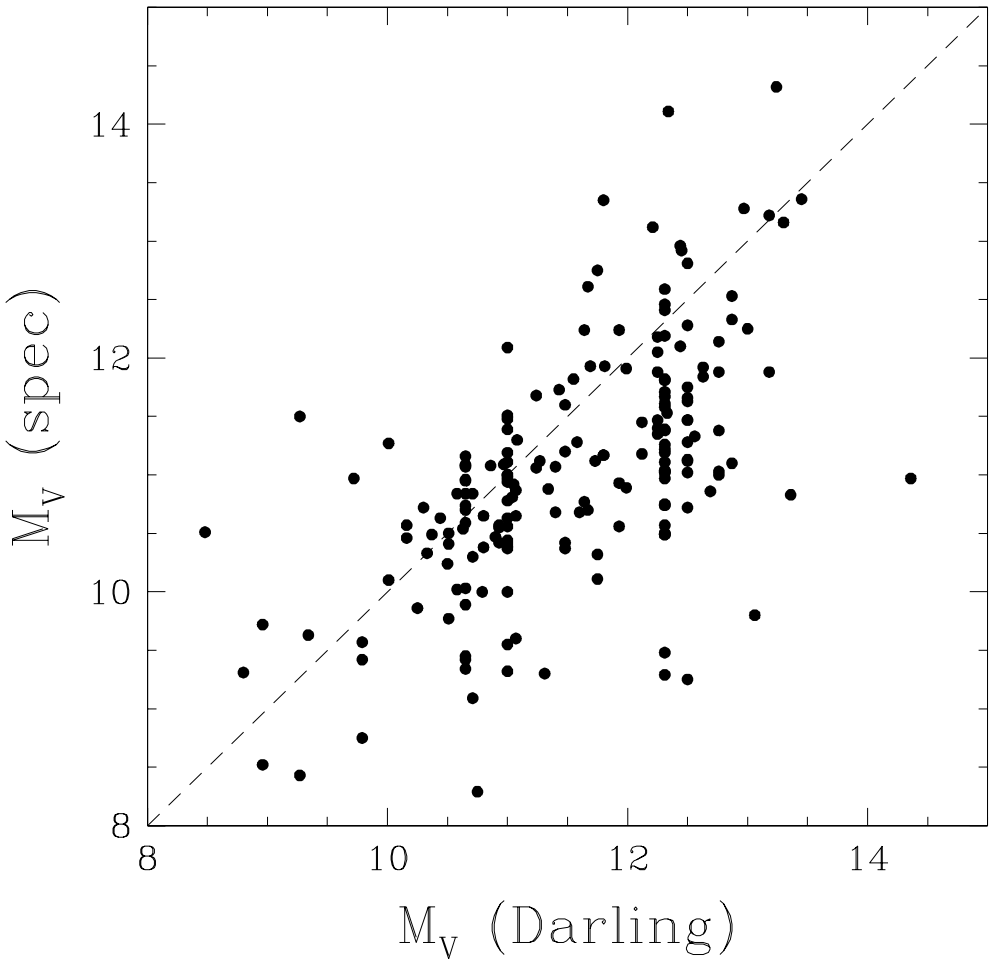

Figure 10

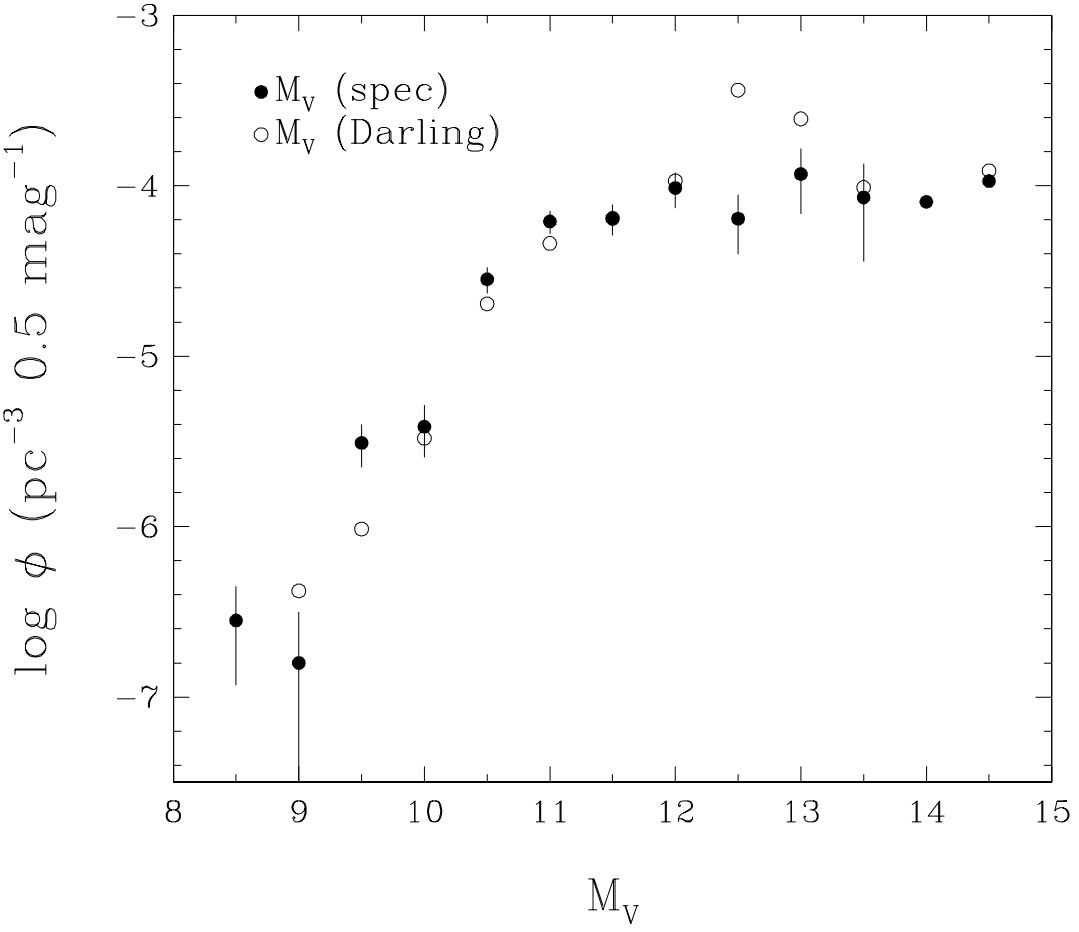

Figure 11

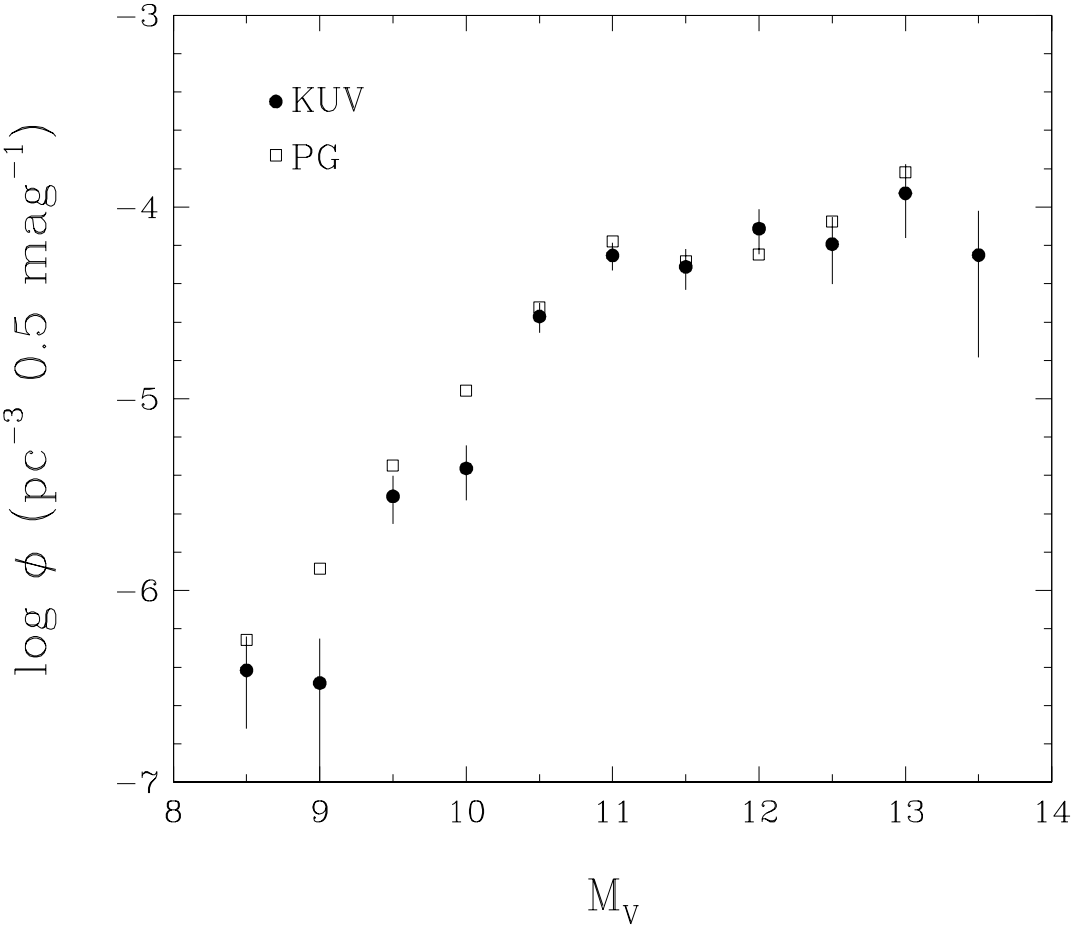

Figure 12

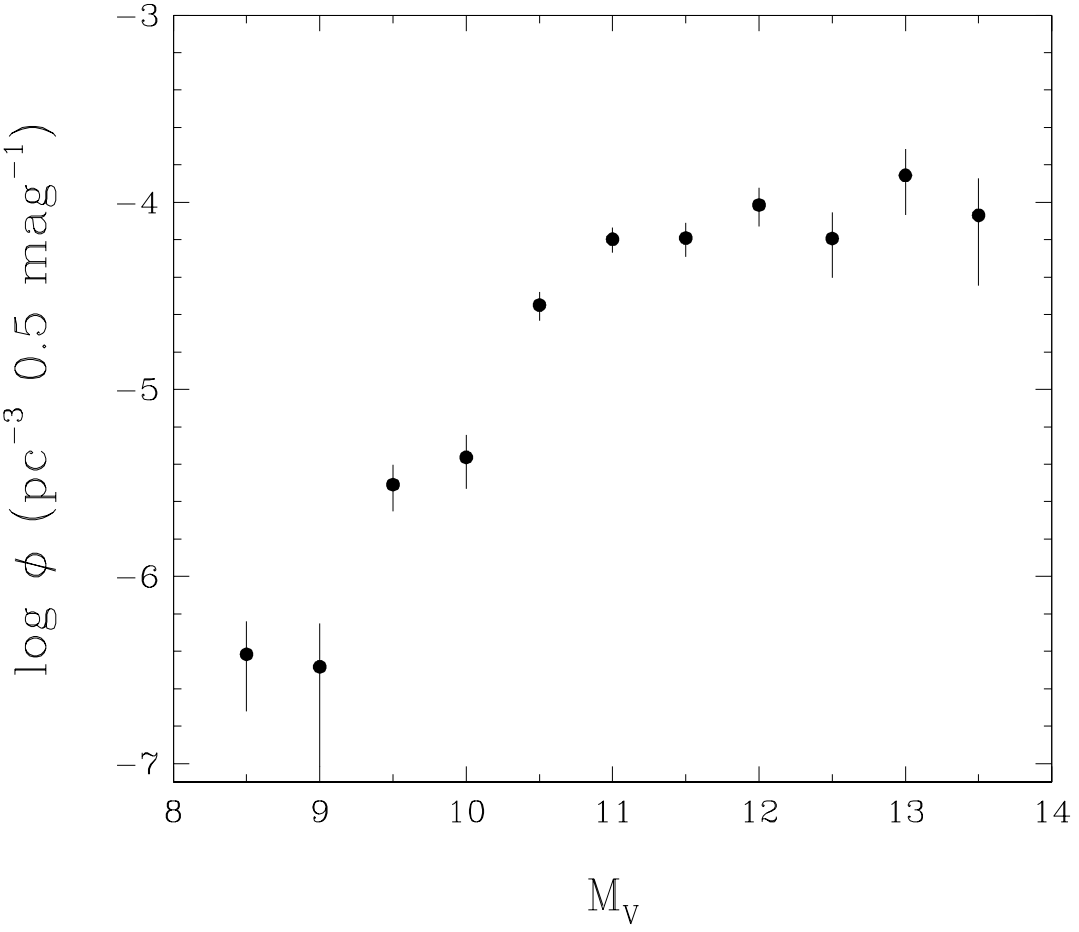

Figure 13

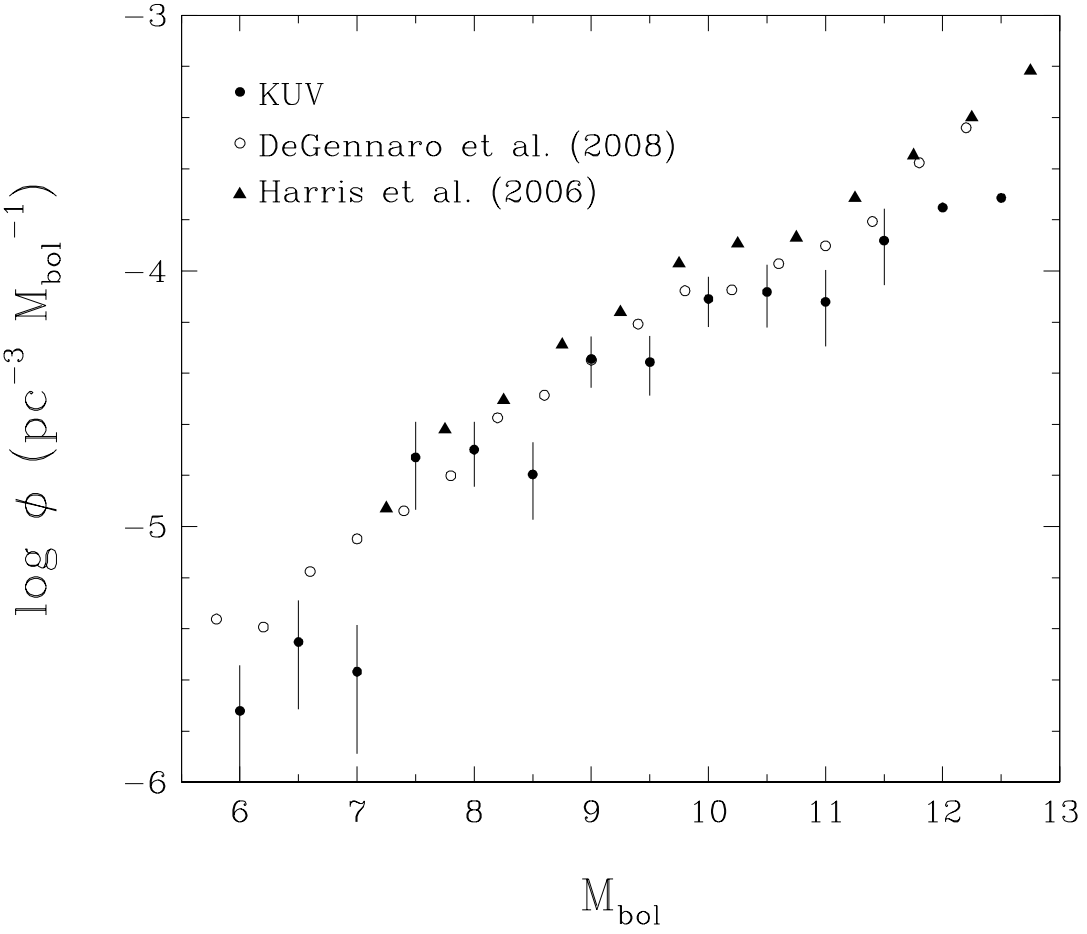
KUV
DeGennaro et al. (2008)
Harris et al. (2006)
log φ (pc^-3 M_bol^-1)
M_bol
−3
−4
−5
−6
6
7
8
9
10
11
12
13

Figure 14